Higher order geometric flows on three dimensional locally homogeneous spaces

Sanjit Das*, Kartik Prabhu†, Sayan Kar‡

Department of Physics & Meteorology *and* Center for Theoretical Studies

Indian Institute of Technology, Kharagpur, 721302, India

Abstract

We analyse second order (in Riemann curvature) geometric flows (un-normalised) on locally homogeneous three manifolds and look for specific features through the solutions (analytic whereever possible, otherwise numerical) of the evolution equations. Several novelties appear in the context of scale factor evolution, fixed curves, phase portraits, approach to singular metrics, isotropisation and curvature scalar evolution. The distinguishing features linked to the presence of the second order term in the flow equation are pointed out. Throughout the article, we compare the results obtained, with the corresponding results for un-normalized Ricci flows.

* Present address: The Institute of Mathematical Sciences, Chennai 600113, India; Electronic address: sanjit@imsc.res.in,

† Present address: Department of Physics, University of Chicago, 5640 S. Ellis Avenue, Chicago, IL 60637, USA; Electronic address: kartikp@uchicago.edu

‡Electronic address: sayan@phy.iitkgp.ernet.in

I. INTRODUCTION AND OVERVIEW

Ricci and other geometric flows [1, 2] were introduced in mathematics by Hamilton [3] and in physics, by Friedan [4], around almost the same time, though with very different motivations. More recently, such geometric flows have become popular, largely because of Perelman's work [5] which led to the proof of the well–known Poincare conjecture. In physics, geometric flows have been investigated in varied contexts such as general relativity, black hole entropy [6] and string theory [7, 8].

The unnormalised Ricci flow equation [1, 2] is given as,

$$\frac{\partial g_{ij}}{\partial t} = -2R_{ij} \tag{1}$$

where g_{ij} is the metric tensor, R_{ij} the Ricci tensor and t denotes a time parameter (not the physical time). For a normalised Ricci flow, the corresponding equation turns out to be:

$$\frac{\partial g_{ij}}{\partial t} = -2R_{ij} + \frac{2}{n}\langle R\rangle g_{ij} \tag{2}$$

where $\langle R\rangle = \frac{\int RdV}{\int dV}$. Thus the normalised flow ceases to be different from the unnormalised one if we consider non–compact, infinite volume manifolds (with a finite value for $\int RdV$). In addition, for constant curvature manifolds, the second term in the normalised flow equation reduces to $\frac{2}{n}Rg_{ij}$.

Friedan's early work showed how one may arrive at the vacuum Einstein field equations of General Relativity from the Renormalisation Group (RG) analysis of a nonlinear σ-model [4]. The RG β-function equations (after a α' dependent scaling of the flow parameter) are given (upto third order in the α' parameter) as follows [9, 10].

$$\frac{\partial g}{\partial t} = -2Rc - \alpha'\widehat{Rc} - 2\alpha'^2\widehat{\widehat{Rc}} - \dots \tag{3}$$

where $\widehat{Rc}$ is a symmetric 2-tensor defined as: $\widehat{Rc} = R_{iklm}R_{jabc}g^{ka}g^{lb}g^{mc}$ and $\widehat{\widehat{Rc}} = \frac{1}{2}R_{klmp}R_i{}^{mlr}R_j{}^{kp}{}_r - \frac{3}{8}R_{iklj}R^{kspr}R^l{}_{spr} + ...$ In component form, we have,

$$\frac{\partial g_{ij}}{\partial \lambda} = -2R_{ij} - \alpha' R_{iklm}R_j{}^{klm} - \dots \tag{4}$$

which may be considered as a *higher order* geometric flow equation for the metric on a given manifold. We intend to continue our investigations [11] on such higher (mainly second) order geometric flow equations, in this article. We mention that apart from a motivational

perspective, our work has no connection with RG flows and, in what follows, we will not discuss any link with them anywhere. α' is treated as a parameter without any link to the RG flow equations. In other words, the higher order flows we talk about are treated as geometric flows in their own right. Restricting to second order we mention a scaling feature of this geometric flow. For Ricci flow a scaling of the metric $g_{ij} \to \Omega g_{ij'}$ can be compensated by a scaling of t by $t' = \frac{t}{\Omega}$. Since the Ricci is invariant under such scaling, flows for g_{ij} and t are equivalent with those for g'_{ij} and t'. For the second order flows, things are a bit different. Here, we can see that flows for g_{ij}, t and α' will be equivalent to flows for g_{ij}/Ω, $t' = t/\Omega$ and $\alpha'' = \alpha'/\Omega$. In our work, we have retained the α' when we do analytic calculations –however, for numerics we have chosen values of $\alpha' = 0, \pm 1$– solutions for other values of α' can be obtained using the scaling property mentioned above.

In this paper, we investigate higher (second) order flows on locally homogeneous three manifolds. After the seminal work of Isenberg and Jackson [12] on the behavior of Ricci flow on homogeneous three manifolds, several interesting papers on this topic have appeared in the literature. Notable among them are the articles in [13], [14], [15], [16], [17]. In particular, the authors in [13] discuss a new approach wherein the Ricci flow of left-invariant metrics on homogeneous three manifolds is equivalently viewed as a flow of the structure constants of the metric Lie algebra w.r.t. an evolving orthonormal frame. Consequences for some other geometric flows on such three manifolds are available in [18],[19].

Homogeneous spaces are also known to play an important role in cosmology in the context of the so–called Bianchi models ([20],[21]). It is worth mentioning that the Misner-Wheeler minisuperspace deals with three dimensional homogeneous spaces in cosmology where different paths in superspace correspond to different evolution profiles for metrics. For more details in this context see [12], [20], [22], [23]. Recently, a connection between self-dual gravitational instantons and geometric flows of all Bianchi types has been shown in [24].

Our article is organised as follows. In Section II, we discuss some preliminaries. Section III reviews the general theory of left invariant metrics. Section IV contains the main results of the article–here we analyse the higher order flows for the various Bianchi classes. Finally, in Section V we conclude with some remarks.

II. PRELIMINARIES ON HOMOGENEOUS THREE MANIFOLDS

Following Isenberg and Jackson[12] (to which we refer for details concerning the following discussion), we take the view point that our original interest is in closed Riemannian 3-manifolds that are locally homogeneous. By a result of Singer [25], the universal cover of a locally homogeneous manifold is homogeneous, i.e. its isometry group acts transitively. Here we begin from the basic definition of homogeneous manifolds and give Thurston's[26] proposition for eight geometric structures. A homogeneous Riemannian space is a Riemannian manifold (M, g) whose isometry group $\mathrm{Isom}(M, g)$ acts transitively on M, i.e given $x, y \in M$ there exists a $\phi \in \mathrm{Isom}(M, g)$ such that $\phi(x) = y$.

If G is a connected Lie group and H is a closed subgroup, G/H is the space of cosets $\{gH\}$, $\pi : G \to G/H$ is defined by $g \to [gH]$. G/H is called a homogeneous space.

Let (M^3, G, G_x) be a maximal model geometry i.e. the isotropy group G_x $(g \in G|gx = x)$ is maximal among all subgroups of the diffeomorphism group of M^3 that have compact isotropy groups. Depending on the isotropy group, there are eight possible manifestations of the maximal model geometry which are also known as Thurston geometries. Here we mention them briefly. If the isotropy group is $SO(3)$ then the model geometry is any one of the three, namely, $SU(2)$, $\mathbb{R}^3$ or $\mathbb{H}^3$. On the other hand, if $SO(2)$ is the isotropy group, then it has four possibilities depending on whether M^3 can be a trivial bundle over a two-dimensional maximal model or not. The first possibility where M^3 is a trivial bundle over a 2-dimensional maximal model, gives rise to $\mathbb{S}^2 \times \mathbb{R}$ or $\mathbb{H}^2 \times \mathbb{R}$ upto diffeomorphism and the latter produces Nil or $\widetilde{SL(2, \mathbb{R})}$ up to isomorphism. The last case where the isotropy group is trivial, the Lie group is isomorphic to Sol.

III. GENERAL THEORY FOR LEFT INVARIANTS METRICS ON 3D UNIMODULAR LIE GROUPS

In studying curvature properties of left invariant metrics on a Lie group, many results have been obtained in the past. Most of them are contained in a survey article by Milnor [27]. For more details on Lie groups and homogeneous spaces we refer to [28], [29] and [30]. We review this work here largely because, later, we will use the results quoted here while writing down the second order geometric flow equations.

The left invariant metric on M^3 is taken as:

$$\begin{aligned} g(t) &= A(t)\eta^1 \otimes \eta^1 + B(t)\eta^2 \otimes \eta^2 + C(t)\eta^3 \otimes \eta^3 \\ &= \pi^1 \otimes \pi^1 + \pi^2 \otimes \pi^2 + \pi^3 \otimes \pi^3 \end{aligned} \tag{5}$$

and its inverse as,

$$\begin{aligned} g^{-1}(t) &= \frac{1}{A(t)}F_1 \otimes F_1 + \frac{1}{B(t)}F_2 \otimes F_2 + \frac{1}{C(t)}F_3 \otimes F_3 \\ &= e_1 \otimes e_1 + e_2 \otimes e_2 + e_3 \otimes e_3 \end{aligned} \tag{6}$$

where $A(t)$, $B(t)$, $C(t)$ are positive. Here $\{F_i\}_{i=1}^3$ are the left invariant frame field (also called Milnor's frame) with dual coframe field $\{\eta^i\}_{i=1}^3$. The Lie brackets w.r.t the left invariant frames are of this form:

$$[F_i, F_j] = \alpha_{ijk}F_k \tag{7}$$

Let us define an orthonormal frame field $\{e_i\}_{i=1}^3$which will be of the form: $e_1 := \frac{1}{\sqrt{A}}F_1$. If we let $\zeta_1 := A, \zeta_2 := B, \zeta_3 := C$ and $\lambda := \alpha_{231}, \mu := \alpha_{312}, \nu := \alpha_{123}$ then Eq.(7) looks like

$$[e_i, e_j] = \frac{\zeta_k \alpha_{ijk}}{\sqrt{\zeta_i\zeta_j\zeta_k}}e_k \tag{8}$$

The relevant components of the sectional curvature turn out to be

$$K(e_1 \wedge e_2) := \langle Rm(e_1, e_2)e_2, e_1\rangle = \frac{(\lambda A - \mu B)^2}{4ABC} + \frac{\nu(2\mu B + 2\lambda A - 3\nu C)}{4AB} \tag{9}$$

$$K(e_2 \wedge e_3) := \langle Rm(e_2, e_3)e_3, e_2\rangle = \frac{(\mu B - \nu C)^2}{4ABC} + \frac{\lambda(2\nu C + 2\mu B - 3\lambda A)}{4BC} \tag{10}$$

$$K(e_3 \wedge e_1) := \langle Rm(e_3, e_1)e_1, e_3\rangle = \frac{(\nu C - \lambda A)^2}{4ABC} + \frac{\mu(2\lambda A + 2\nu C - 3\mu B)}{4AC} \tag{11}$$

Recall that these are actually R_{1212}, R_{2323}, R_{3131}, respectively, in the orthonormal frame. We have to write them back in Milnor's frame. Thus the Riemann tensor in the Milnor frame will be

$$Rm(F_i, F_j, F_i, F_j) = \zeta_i\zeta_j Rm(e_i, e_j, e_i, e_j) \tag{12}$$

From now on we would mean:$\langle Rm(e_i, e_j)e_j, e_i\rangle = Rm(e_i, e_j, e_i, e_j)$. Similarly the Ricci and $\widehat{Rc}$ would look as :

$$Rc(F_i, F_i) = \sum_{k=1}^{3} Rm(F_i, F_k, F_i, F_k)\frac{1}{\zeta_k} \tag{13}$$

$$\widehat{\mathrm{Rc}(F_i,F_i)} = 2\sum_{k=1}^{3} Rm(F_i,F_k,F_i,F_k)^2 \frac{1}{\zeta_k^2}\frac{1}{\zeta_i} \tag{14}$$

$$\begin{aligned}
\mathrm{Rc}(F_1,F_1) &= \frac{(\lambda A)^2-(\mu B-\nu C)^2}{2BC} && (15)\\
\mathrm{Rc}(F_2,F_2) &= \frac{(\mu B)^2-(\nu C-\lambda A)^2}{2CA} && (16)\\
\mathrm{Rc}(F_3,F_3) &= \frac{(\nu C)^2-(\lambda A-\mu B)^2}{2AB} && (17)
\end{aligned}$$

$$\begin{aligned}
\widehat{\mathrm{Rc}(F_1,F_1)} &= \frac{1}{8AB^2}\left[\frac{(\lambda A-\mu B)^2}{C}+\nu(2\mu B+2\lambda A-3\nu C)\right]^2\\
&\quad+\frac{1}{8AC^2}\left[\frac{(\nu C-\lambda A)^2}{B}+\mu(2\lambda A+2\nu C-3\mu B)\right]^2 && (18)\\
\widehat{\mathrm{Rc}(F_2,F_2)} &= \frac{1}{8BC^2}\left[\frac{(\mu B-\nu C)^2}{A}+\lambda(2\nu C+2\mu B-3\lambda A)\right]^2\\
&\quad+\frac{1}{8BA^2}\left[\frac{(\lambda A-\mu B)^2}{C}+\nu(2\mu B+2\lambda A-3\nu C)\right]^2 && (19)\\
\widehat{\mathrm{Rc}(F_3,F_3)} &= \frac{1}{8A^2C}\left[\frac{(\nu C-\lambda A)^2}{B}+\mu(2\lambda A+2\nu C-3\mu B)\right]^2\\
&\quad+\frac{1}{8B^2C}\left[\frac{(\mu B-\nu C)^2}{A}+\lambda(2\nu C+2\mu B-3\lambda A)\right]^2 && (20)
\end{aligned}$$

Using the above expressions, we can calculate the scalar curvature and the norm of the Ricci tensor which are given as,

$$\begin{aligned}
\mathrm{Scal} &= \frac{1}{A}\left(\mathrm{Rc}(F_1,F_1)\right) + \frac{1}{B}\left(\mathrm{Rc}(F_2,F_2)\right) + \frac{1}{C}\left(\mathrm{Rc}(F_3,F_3)\right) && (21a)\\
&= -\frac{A^2\lambda^2+(B\mu-C\nu)^2-2A\lambda(B\mu+C\nu)}{2ABC} && (21b)
\end{aligned}$$

$$\begin{aligned}
\|\mathrm{Rc}\|^2 &= \frac{1}{A^2}\left(\mathrm{Rc}(F_1,F_1)\right)^2 + \frac{1}{B^2}\left(\mathrm{Rc}(F_2,F_2)\right)^2 + \frac{1}{C^2}\left(\mathrm{Rc}(F_3,F_3)\right)^2 && (22a)\\
&= \frac{3A^4\lambda^4-4A^3\lambda^3(B\mu+C\nu)-4A\lambda(B\mu-C\nu)^2(B\mu+C\nu)+2A^2\lambda^2(B\mu+C\nu)^2}{4A^2\ B^2\ C^2}\\
&\quad+\frac{(B\mu-C\nu)^2\left(3B^2\mu^2+2BC\mu\nu+3C^2\nu^2\right)}{4A^2\ B^2\ C^2} && (22b)
\end{aligned}$$

The higher order flow equations therefore turn out to be,

$$\frac{dA}{dt} = -\Big(2\mathrm{Rc}(F_1,F_1) + \alpha' \widehat{\mathrm{Rc}(F_1,F_1)}\Big) \tag{23}$$
$$\frac{dB}{dt} = -\Big(2\mathrm{Rc}(F_2,F_2) + \alpha' \widehat{\mathrm{Rc}(F_2,F_2)}\Big) \tag{24}$$
$$\frac{dC}{dt} = -\Big(2\mathrm{Rc}(F_3,F_3) + \alpha' \widehat{\mathrm{Rc}(F_3,F_3)}\Big) \tag{25}$$

In the next section we analyze the flow equations in five different homogeneous spaces.

IV. EXAMPLES ON BIANCHI CLASSES

A. Computation on SU(2)

1. Flow equations

The canonical three sphere (S^3) is topologically equivalent to the Lie group $SU(2)$, which is algebraically represented by

$$SU(2) = \left\{ \begin{pmatrix} z_1 & -z_2 \\ \bar{z_2} & \bar{z_1} \end{pmatrix} : z_1, z_2 \in \mathbb{C}, \quad |z_1|^2 + |z_2|^2 = 1 \right\}. \tag{26}$$

All the structure constants are the same in the Milnor frame field. We assume $\lambda = \mu = \nu = -2$. With these values of the structure constants, the $2nd$ order flow equations turn out to be:

$$\frac{dA}{dt} = \frac{4(B-C)^2 - 4A^2}{BC} - 2\alpha'[\frac{1}{AB^2}\{\frac{(A-B)^2}{C} + (2B+2A-3C)\}^2 + \frac{1}{AC^2}\left\{\frac{(A-C)^2}{B} + (2C+2A-3B)\right\}^2] \tag{27}$$

$$\frac{dB}{dt} = \frac{4(C-A)^2 - 4B^2}{AC} - 2\alpha'[\frac{1}{BC^2}\{\frac{(C-B)^2}{A} + (2C+2B-3A)\}^2 + \frac{1}{BA^2}\{\frac{(B-A)^2}{C} + (2B+2A-3C)\}^2] \tag{28}$$

$$\frac{dC}{dt} = \frac{4(A-B)^2 - 4C^2}{AB} - 2\alpha'[\frac{1}{CA^2}\{\frac{(A-C)^2}{B} + (2A+2C-3B)\}^2 + \frac{1}{CB^2}\{\frac{(C-B)^2}{A} + (2C+2B-3A)\}^2] \tag{29}$$

2. Analytical and numerical estimates

We first try and see if we can analytically estimate the nature of evolution for the scale factors A, B, and C.

(a) Without any loss of generality, we can take the initial values of the scale factors in an ordered way i.e. $A_0 > B_0 > C_0$. Further, from Eqn.27 to 29 we can write the equations for the differences (pairwise) of the scale factors as follows.

$$\frac{d(A-B)}{dt} = -4\frac{(A-B)\,(A^2+2AB+B^2-C^2)}{ABC} - 4\alpha'\frac{(A-B)\;\mathcal{G}_1(A,B,C)}{A^2B^2C^2} \tag{30}$$

$$\frac{d(A-C)}{dt} = -4\frac{(A-C)\,(A^2+2AC+C^2-B^2)}{ABC} - 4\alpha'\frac{(A-C)\;\mathcal{G}_2(A,B,C)}{A^2B^2C^2} \tag{31}$$

$$\frac{d(B-C)}{dt} = -4\frac{(B-C)\,(B^2+2BC+C^2-A^2)}{ABC} - 4\alpha'\frac{(B-C)\;\mathcal{G}_3(A,B,C)}{A^2B^2C^2} \tag{32}$$

where $\mathcal{G}_1(A,B,C),\ \mathcal{G}_2(A,B,C),\ \mathcal{G}_3(A,B,C)$ are, respectively

$$\begin{aligned}\mathcal{G}_1(A,B,C) = \big(&A^4-4A^3B+6A^2B^2-4AB^3+B^4\\ &+2A^2C^2+12ABC^2+2B^2C^2-8AC^3-8BC^3+5C^4\big)\end{aligned} \tag{33}$$

$$\begin{aligned}\mathcal{G}_2(A,B,C) = \big(&A^4+2A^2B^2-8AB^3+5B^4-4A^3C\\ &+12AB^2C-8B^3C+6A^2C^2+2B^2C^2-4AC^3+C^4\big)\end{aligned} \tag{34}$$

$$\begin{aligned}\mathcal{G}_3(A,B,C) = \big(&5A^4-8A^3B+2A^2B^2+B^4-8A^3C\\ &+12A^2BC-4B^3C+2A^2C^2+6B^2C^2-4BC^3+C^4\big)\end{aligned} \tag{35}$$

From the above expressions for the differences, it can be inferred that $A(t) > B(t) > C(t)$ holds throughout the evolution, if the initial values satisfy $A_0 > B_0 > C_0$. Note that each of (30)-(32) may be formally solved. For example, if we consider (31), we have $A(t) - C(t) = (A_0 - C_0)\exp\left[\int \mathcal{K}(t')dt'\right]$.

(b) We now look at the evolution of $B(t)$ for $\alpha' = +1$. We have, from Eqn.28,

$$\frac{dB}{dt} = 4\frac{(A^2+C^2)}{AC} - 2\{\frac{B^2}{AC}+\frac{P_1}{BC^2}+\frac{P_2}{BA^2}+4\} \leq 4\frac{(A^2+C^2)}{AC} - 2\{\frac{B}{A}+\frac{P_1}{BC^2}+\frac{P_2}{BA^2}+4\} \tag{36}$$

where $P_1 = \{\frac{(C-B)^2}{A} + (2C + 2B - 3A)\}^2$ and $P_2 = \{\frac{(A-B)^2}{C} + (2B + 2A - 3C)\}^2$ are strictly positive. Choosing $A_0 = n+2, B_0 = n, C_0 = n-2$ as the initial values of the scale factors, it can be shown that $\frac{dB}{dt}\big|_{t=t_0}$ is always negative (from the inequality above, it may be checked that the negative term always dominates over the positive term). Further, it is easy to see that for $n > 4$ and $\alpha' = (0, +1)$, all the scale factors are decreasing.

(c) On the other hand, for $\alpha' = -1$ the upper bound on $B(t)$ can be written as

$$\frac{dB}{dt} \leq -4\frac{B}{A} + \frac{4(A-C)^2}{AC} + 2\frac{P_1}{BC^2} + 2\frac{P_2}{BA^2} \tag{37}$$

Here we may note a difference with the $\alpha' = +1$ case. As before, let us choose $A_0 = n+2, B_0 = n, C_0 = n-2$ to estimate $F_1 = -4\frac{B}{A} + \frac{4(A-C)^2}{AC} + 2\frac{P_1}{BC^2} + 2\frac{P_2}{BA^2}$ which turns out to be, $F_1 = \frac{4(256+n(-64+n(24+n(20-(-3+n)n))))}{n(n^2-4)^2}$. It is easy to see that F_1 is bounded below (i.e.$\lim_{n\to\infty} F_1 = -4$ and for any finite n, F_1 is larger than -4.). Thus, the scale factor $B(t)$ can either decrease or increase depending on the choice of initial values.

(d) It is easy to see from the flow equations that for $\alpha' = (0, -1)$, $A(t)$, $B(t)$ and $C(t)$ will monotonically decrease when $A > (B - C)$. For typical initial values obeying this condition, this decreasing feature is shown in Fig. 1(a)and Fig.1(d) where $A(t), B(t)$ and $C(t)$ are obtained by numerically solving the dynamical system. In the graphs, $A(t)$, $B(t)$ and C(t)) are shown in thick, dashed and dotted lines, respectively. We follow this convention in our plots, throughout this article.

(e) We now ask whether all the scale factors can be increasing in t. For $\alpha' = 0$ this is not possible. To see this, consider the initial value assumption $A_0 > B_0 > C_0$. The scale factor $A(t)$ will increase for $A < (B - C)$, whereas both $B(t)$ and $C(t)$ will increase for $A > (B + C)$. However, both these inequalities cannot hold simultaneously. Hence all scale factors cannot be increasing in t.

For $\alpha' = -1$ we may be tempted to believe in a conclusion similar to the $\alpha' = 0$ case mentioned above. However, the higher order contribution leads to some unexpected behaviour. In Fig.1(c) we see that the scale factor $B(t)$ initially increases but eventually decreases after a certain time. This is due to the the fact that the $A > (B + C)$ criterion does not hold in the entire domain of t, a fact apparent from the figure. In contrast, for Fig.1(b) we have

taken initial values which do not satisfy the aforesaid condition and though, initially, $B(t)$ is decreasing we find that after some time, $B(t)$ increases. The reason behind this behaviour is — the higher order contribution is much more positive and the net effect makes $B(t)$ increase after an initial decreasing phase.

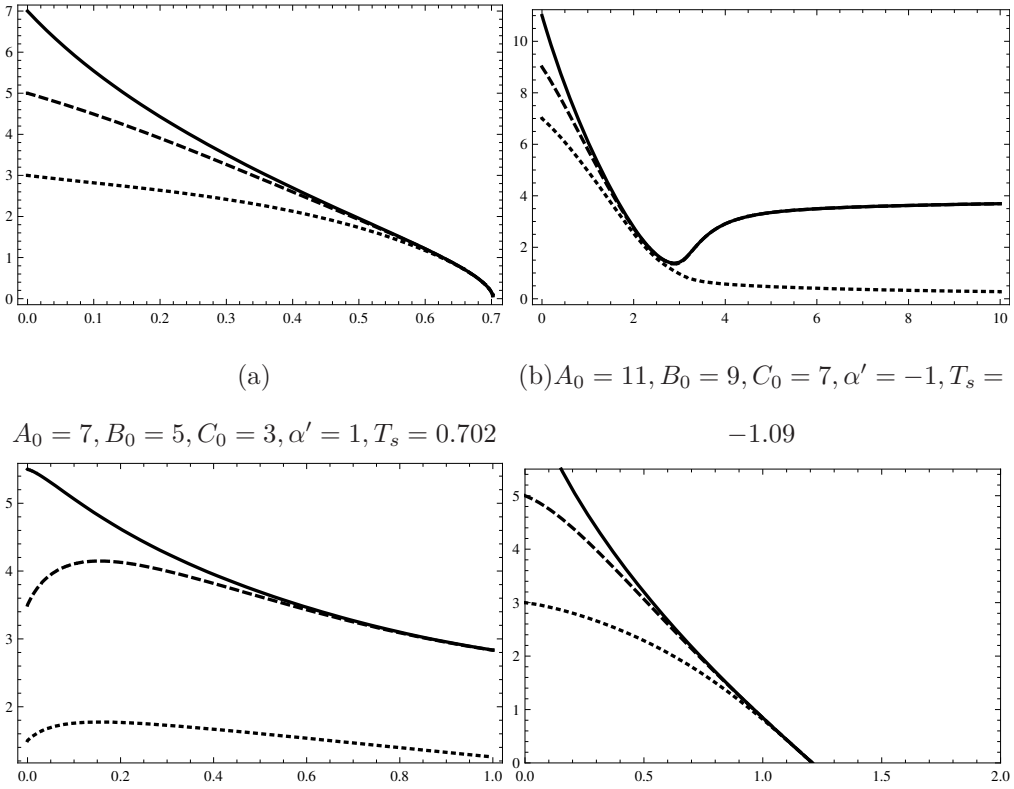

(a) $A_0 = 7, B_0 = 5, C_0 = 3, \alpha' = 1, T_s = 0.702$

(b) $A_0 = 11, B_0 = 9, C_0 = 7, \alpha' = -1, T_s = -1.09$

(c) $A_0 = 5.5, B_0 = 3.5, C_0 = 1.5, \alpha' = -1, T_s = -0.04$

(d) $A_0 = 7, B_0 = 5, C_0 = 3, \alpha' = 0, T_s = 2.76$

Figure 1: $A(t), B(t), C(t)$ vs t for $\alpha' = 1$, $\alpha' = -1$ and $\alpha' = 0$ for SU(2)

(f) recall that $SU(2)$ admits round Einstein metrics and the Ricci flow converges. This feature remains even when we include higher order terms with $\alpha' = 1$. If we change the value of α'(from 1 to 0) a change appears only in the singularity time, though no difference appears in the nature of the graph. On the other hand, when $\alpha' = -1$, we notice an expansion of the scale factors – $B(t)$ and $A(t)$ appear to be expanding beyond the minimum in Fig.[1(b)] at the same rate, whereas $C(t)$ goes to zero asymptotically.

Let us now move on to some special cases.

3. **Special Case:** $A \neq B = C$

The flow equations, with this restriction (leading to the so-called Berger sphere metrics [1]) become,

$$\frac{dA}{dt} = -4\frac{A^2}{B^2} - 4\alpha' \frac{A^3}{B^4} \tag{38}$$

$$\frac{dB}{dt} = -8 + 4\frac{A}{B} - 4\alpha' \left[\frac{5}{B}(\frac{A}{B} - 1)^2 + \frac{3}{B}(1 - \frac{2A}{3B})\right] \tag{39}$$

Let us first look at the case, $\alpha' = 0$. It is clear from Eqn. (38) that $A(t)$ decreases with t and has a upper bound, $A(t) \leq A_0 - 4t$. However, the same is not true for $B(t)$. If $A(t) < 2B(t)$ then $B(t)$ decreases with increasing t, otherwise it increases. $B(t)$ does have a lower bound, $B(t) \geq B_0 - 8t$. Depending on the sign of the R. H. S. of (39) $B(t)$ can have an increasing, stationary or decreasing behaviour during its evolution in t. From Eqns. (38), (39), one can arrive at a second order equation for $B(t)$ given as:

$$B(t)\frac{d^2B}{dt^2} + 2\left(\frac{dB(t)}{dt}\right)^2 + 24\frac{dB(t)}{dt} = -64 \tag{40}$$

There are trivial solutions to this equation: $\frac{dB(t)}{dt} = -8$ (which corresponds to $A(t) = 0$) and $\frac{dB(t)}{dt} = -4$ (which corresponds to $A(t) = B(t)$). If we define $\frac{dB}{dt} = D(t)$ then we can see the following: (i) At some t if $D = 0$ then $\frac{dD}{dt} < 0$ (maximum); (ii) If, over a range of t, $D > 0$ then $\frac{dD}{dt} < 0$; (iii) If, over a range of t, $D < 0$ then $\frac{dD}{dt}$ can be < 0, > 0 or $= 0$. We note this behaviour in Fig.2(d). For example, the maximum occurs at the point where $D(t) = 0$–substitute the values of $A(t)$ and $B(t)$ at the maximum as found in the graph, into Eqn. (39) (with $\alpha' = 0$) and check that it is indeed zero.

Now we wish to note what happens to the rate of change of $(A - B)$ and $(A + B)$. We show that $(A - B)$ decreases faster than $(A + B)$ which implies that as A and B decrease, they approach each other. From the above equations for $\alpha' = 0$ we can write

$$\frac{d(A-B)}{dt} = \frac{-4(A+2B)}{B^2}(A-B) \leq -\frac{4A}{B^2}(A^2 + 3AB + B^2) \leq -20\frac{A}{B} \tag{41}$$

On the other hand,

$$\frac{d(A+B)}{dt} = -\frac{4}{B^2}(A^2 + 2B^2) + 4\frac{A}{B} \leq -4\frac{A}{B} \tag{42}$$

It is easy to note that $A - B$ decreases faster than $A + B$. Thus A and B approach each other while decreasing. For $\alpha' \neq 0$ the analysis can be done following similar logic but we prefer to solve the equations numerically and demonstrate our conclusions.

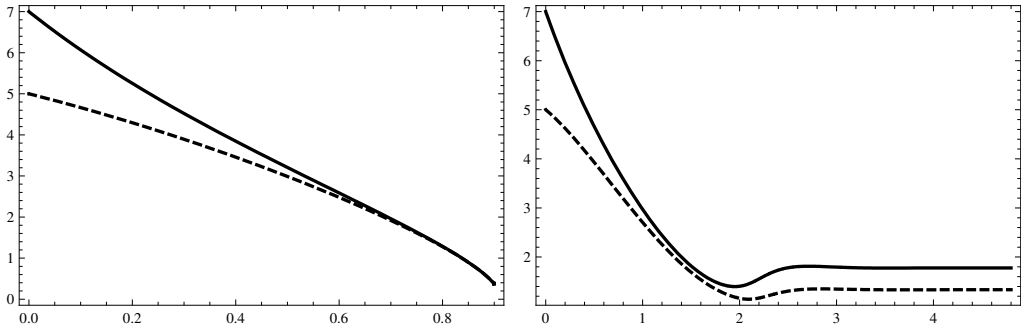

(a)$A_0 = 7, B_0 = 5, \alpha' = 1, T_s = 0.914$ (b)$A_0 = 7, B_0 = 5, \alpha' = -1, T_s = -0.602$

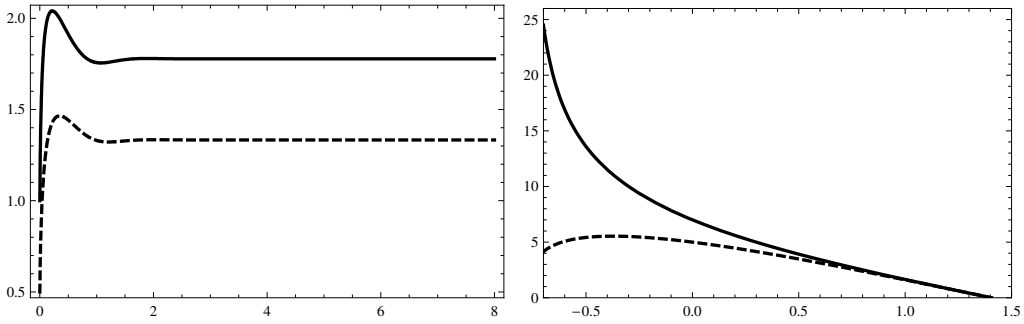

(c)$A_0 = 1, B_0 = 0.5, \alpha' = -1, T_s = -0.004$ (d)$A_0 = 7, B_0 = 5, \alpha' = 0, T_s = (-0.76)$

Figure 2: $A(t), B(t)$ vs t for $\alpha' = 1$, $\alpha' = -1$ and $\alpha' = 0$ for SU(2)

If we plot $A(t)$ (thick line), $B(t)$ (dashed line) treating the evolution equations as a dynamical system, we see that both the scale factors converge to the origin (Fig.2(a),2(d)) for $\alpha' = 0, 1$. However, for $\alpha' = -1$ the evolution of the scale factors depend entirely on the initial values of A, B, C– a fact shown in the two figures, Fig.2(b),2(c).

4. Phase plots

We obtain phase plots of the above dynamical system in Fig.3. The curves are the trajectories of the system for varying initial conditions, and the arrows indicate the direction of increasing time. From the phase plots we can deduce the qualitative and quantitative behaviour of the flow. We can see that the $A = B$ line is a critical curve demarcating the regions in phase space with different behaviour. Also, for $\alpha' = 0$ all flow trajectories converge towards the $A = B$ line. This leads to isotropization of the manifold. However, for $\alpha' = 1$, trajectories from a region in the phase space with $A > B$ converge to the singularity $B = 0$ before isotropization. The behaviour for $\alpha' = -1$ is markedly different due to the existence of fixed points given by $(A, B) = (0, 4), (\frac{16}{9}, \frac{4}{3}), (1, 1)$. In this case, trajectories

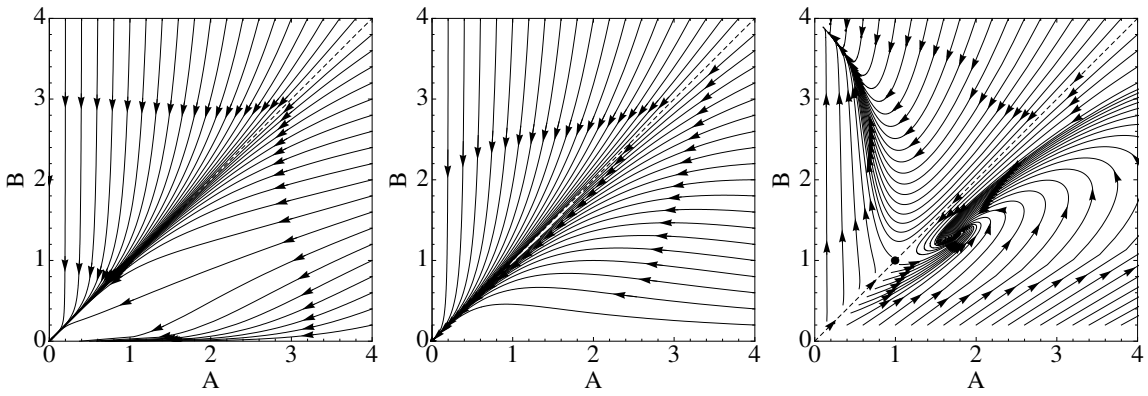

(a)$\alpha' = 1$ (b)$\alpha' = 0$ (c)$\alpha' = -1$

Figure 3: $2nd$ order flow on SU(2)for $B = C$

from $A > B$ converge to $(\frac{16}{9}, \frac{4}{3})$ and those from $A < B$ converge to $(0, 1)$. When $A = B$, we note a convergence to $(1, 1)$. Therefore, in this case there is no isotropization, with the asymptotic manifold being non-isotropic - a fact which is manifest in the values of the fixed points.

5. Curvature evolution

Finally, we show the evolution of the scalar curvature. From Eqn.[21b] and Eqn.[22b] we can immediately compute the scalar curvature or norm of the Ricci tensor, for locally homogeneous three manifolds in the different Bianchi classes. These quantitites depend on the scale factors. Thus, if we know the behaviour of the scale factors, under a given flow, we can easily obtain the profile of any curvature invariant as a function of the flow parameter. However, in most cases, we do not have exact solutions for the scale factors. Therefore, the numerical evaluations of the scale factors (for various initial values) are used to obtain the curvature invariants. From Eqn.21b we can see, for $SU(2)$, the scalar curvature is as follows

$$\text{Scal} = \frac{-2\left[A^2 + (B+C)^2 - 2A(B+C)\right]}{ABC} = \frac{2\ F(A,B,C)}{ABC} \tag{43}$$

Therefore, it can be positive, negative or zero depending on the values of A, B, C. More specifically if $A = B = C$ then $F = 3A^2 > 0$. Similarly if we take $A \neq B = C$ then $F = A(4B - A)$, which can be zero, negative or positive for $A = 4B$, $A > 4B$ or $A < 4B$ respectively.

Fig. 4 shows the profiles for the scalar curvature. For different initial values and three

different α' we have shown the evolution. Both $\alpha' = 0$ and $\alpha' = 1$ show a monotonic nature of the scalar curvature. For $\alpha' = -1$ the scale factors are not always monotonic – the behavior depends on the initial conditions. The scalar curvature for $\alpha' = -1$ rises initially but asymptotically reaches a constant value. The figures in the first row, second column and in the third row, second column show the appearance of negative scalar curvature. We note here that *Scal* remains entirely negative or entirely positive during evolution, for $\alpha' = 0, 1$, but may grow from negative to positive value for $\alpha' = -1$.

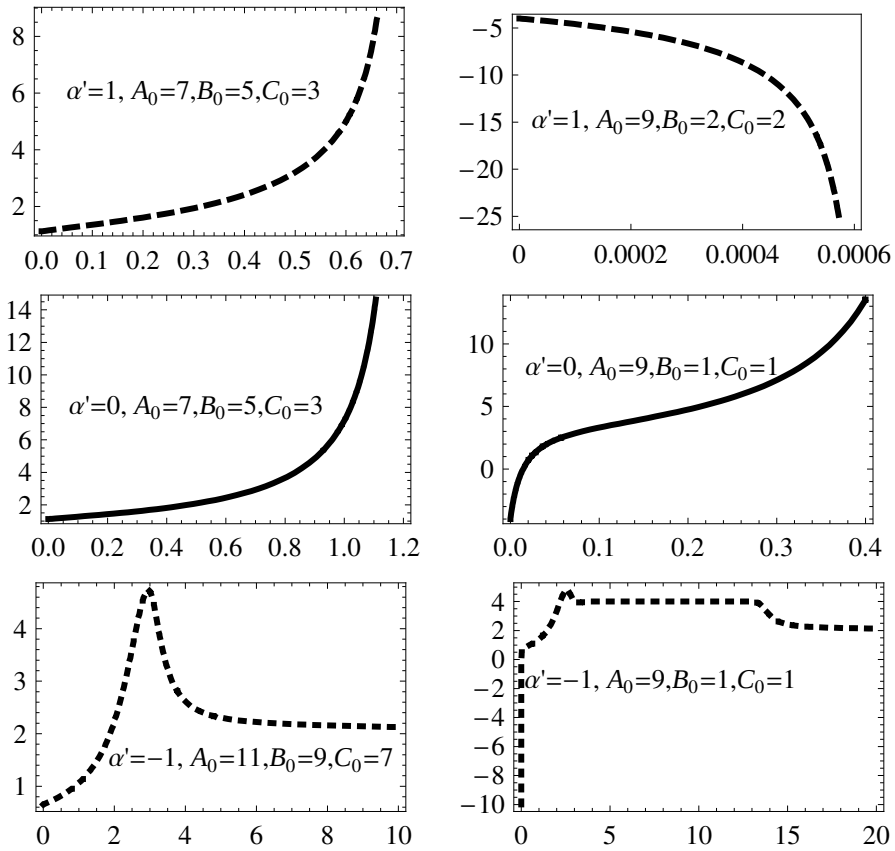

Figure 4: Evolution of Scal for $SU(2)$.

In summary, several distinguishing features of scale factor evolution and curvature evolution arising exclusively due to the presence of the higher order term in the flow, have been pointed out in the above analysis and summarised in Table I.

Table I: Comparison of the evolution of different scale factors and Scal. curvature for $SU(2)$

	$A(t)$	$B(t)$	$C(t)$	$Scal$
$\alpha' = 0$	decreasing	decreasing	decreasing	increases, can be -ve.
$\alpha' = 1$	decreasing much faster	decreasing much faster	decreasing much faster	increase/decrease (entirely +ve or -ve.)
$\alpha' = -1$	depending on initial value	depending on initial value	decreasing	not monotonic (can be +ve, -ve)

B. Computation on Nil

1. Flow equations

Nil is a three dimensional Lie group consisting of all 3×3 matrices of the form

$$\begin{pmatrix} 1 & x & z \\ 0 & 1 & y \\ 0 & 0 & 1 \end{pmatrix}$$

under multiplication, also known as the Heisenberg group. The group action in $\mathbb{R}^3$ can be written as

$$(x, y, z) \circ (x', y', z') = (x + x', y + y', z + z' + xy') \tag{44}$$

This is a nilpotent group. We can put a left invariant frame field on this Lie group. With the inherent metric, †it is a line bundle over the Euclidean plane $\mathbb{E}^2$. Following Milnor [27] we have the structure constants, $\lambda = -2, \mu = \nu = 0$. The Rc and $\widehat{Rc}^2$ tensors can be obtained by simple computation. The flow equations in this case will be:

$$\frac{dA}{dt} = -\frac{4A^2}{BC} - 4\alpha' \frac{A^3}{B^2C^2} \tag{45}$$

$$\frac{dB}{dt} = \frac{4A}{C} - 20\alpha' \frac{A^2}{BC^2} \tag{46}$$

[†] One such left invariant metric is $ds^2 = dx^2 + dy^2 + (dz - xdy)^2$.

$$\frac{dC}{dt} = \frac{4A}{B} - 20\alpha' \frac{A^2}{B^2 C} \tag{47}$$

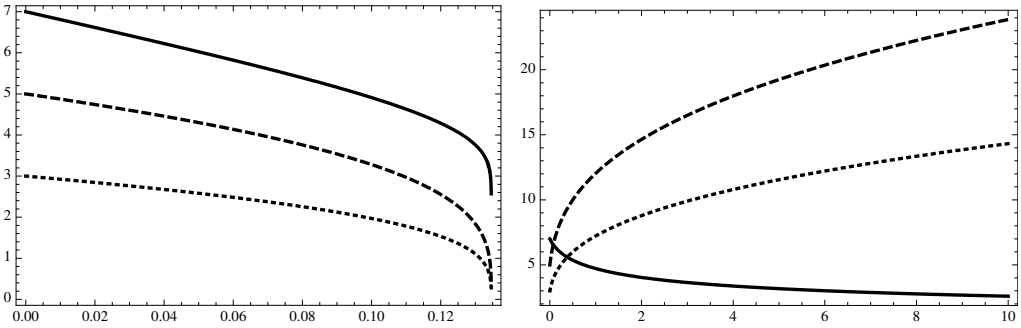

(a)

$(A_0, B_0, C_0) = (7, 5, 3), \alpha' = 1, T_s = 0.134$

(b)$(A_0, B_0, C_0) = (7, 5, 3), \alpha' = -1, T_s = -0.043$

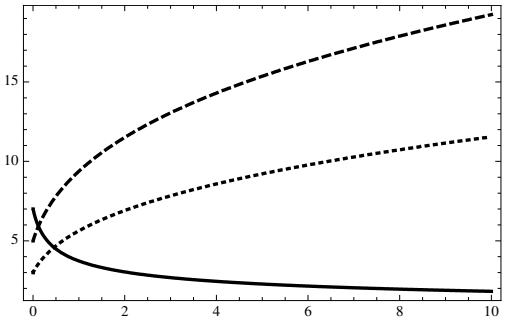

(c)

$(A_0, B_0, C_0) = (7, 5, 3), \alpha' = 0, T_s = -0.17$

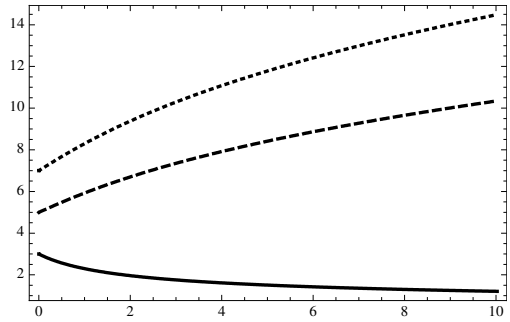

(d)$(A_0, B_0, C_0) = (3, 5, 7), \alpha' = 1$

Figure 5: $A(t), B(t), C(t)$ vs t for $\alpha' = 1$and $\alpha' = 0$ for Nil

2. **Numerical estimates**

First we solve the flow equations numerically and look for specific characteristics of the flow for different types of initial conditions. In Fig.5(a) we see that for $\alpha' = 1$, $A_0 \geq B_0 \geq C_0$ and $A_0, B_0, C_0 \geq 1$ the flow converges in every direction, contrary to unnormalized Ricci flow (Fig.5(c)) where the B, C are expanding and diverge diverge while $(A(t))$ converges i.e. a pancake degeneracy exists (the same happens for normalized Ricci flow as mentioned in[12]). Further, for $\alpha' = 0$ (Fig. 5(b)) and any value of $A(t), B(t), C(t)$, the flow has a past singularity. For $\alpha' = 1$, if $A_0 \leq B_0 \leq C_0$ the evolution of the scale factors resemble the unnormalized Ricci flow but have no singularity. On the other hand, for $\alpha' = -1$ (Fig.5(b)) and any value of $A(t)$, $B(t)$, $C(t)$, the flow has a past singularity, similar to $\alpha' = 0$ case.

3. **Analytical solution**

It is possible to solve the flow equations analytically. Before working out the solutions, we note from the flow equations that $B/C =$ constant. Let us now choose a new variable $\xi = BC/A$. It can be shown easily [31] that, with this choice and appropriate scaling of the coordinates, the nature of the flow can be determined entirely by finding the evolution of ξ. In other words, Nil has a one dimensional family of left invariant metrics which is parametrised by ξ. The flow equations now take the form

$$\dot{\xi} = 12 - \alpha' \, \frac{36}{\xi} \tag{48a}$$

$$\frac{\dot{A}}{A} = -\frac{4}{\xi}\left(1 + \alpha' \, \frac{1}{\xi}\right) \tag{48b}$$

$$\frac{\dot{B}}{B} = \frac{4}{\xi}\left(1 - \alpha' \, \frac{5}{\xi}\right) \tag{48c}$$

where the ξ equation replaces the C equation and A, B are functions of ξ. So, effectively, there is only one scale factor to worry about, i.e. ξ. The ξ equation is readily solved to give two solutions–

$$\xi + 3\alpha' \, \ln|\xi - 3\alpha'| = 12t + k \tag{49a}$$

OR

$$\xi = 3\alpha' \tag{49b}$$

The equations for A and B can then be solved to obtain $A(\xi)$ and $B(\xi)$given as,

$$\frac{A}{A_0} = \left(\frac{\xi}{\xi_0}\right)^{\frac{1}{9}} \left(\frac{\frac{\xi}{3} - \alpha'}{\frac{\xi_0}{3} - \alpha'}\right)^{\frac{-4}{9}} \qquad \& \qquad \frac{B}{B_0} = \left(\frac{\xi}{\xi_0}\right)^{\frac{1}{45}} \left(\frac{\frac{\xi}{3} - \alpha'}{\frac{\xi_0}{3} - \alpha'}\right)^{\frac{-2}{225}} \tag{50a}$$

$$A = A_0 \exp\left(-\frac{16}{3\alpha'}t\right) \qquad \& \qquad B = B_0 \exp\left(-\frac{8}{3\alpha'}t\right) \tag{50b}$$

where (49a) is for the ξ given in (48a) and (49b) corresponds to the solution (48b). The evolution of C can also be found using $C = \frac{A\xi}{B}$. In the case $\alpha' = 1$, and $\xi = 3\alpha'$ we can easily see that the scale factors $A(t)$, $B(t)$ and $C(t)$ decrease. When $\alpha' = 0$, $\xi = 12t$ and $A(t) \sim t^{-\frac{1}{3}}$, $B(t) \sim t^{\frac{1}{3}}$, $C(t) \sim t^{\frac{1}{3}}$. For $\alpha' = -1$, the solution $\xi = 3\alpha'$ is not valid as long as

we are dealing with Riemannian manifolds and the evolution is determined from the other solution.

Next we move on to a special case where $B = C$.

4. **Special Case:** $A \neq B = C$

The flow equations, under this assumption are

$$\begin{cases} \frac{dA}{dt} = -\frac{4A^2}{B^2} - 4\alpha' \frac{A^3}{B^4} \\ \frac{dB}{dt} = \frac{4A}{B} - 20\alpha' \frac{A^2}{B^3} \end{cases} \tag{51}$$

It is obvious that the same analytical solutions mentioned above are valid here as long as we define $\xi = \frac{B^2}{A}$. However, we discuss some alternative ways of arriving at the nature of scale factor evolution.

Let us look at the difference between the scale factors given as

$$\frac{d(A-B)}{dt} = -4\frac{A}{B^2}(A+B) - 4\alpha'(\frac{A}{B^2})^2(A-5B) \leq -4\frac{A}{B^2}(A-B) - 4\alpha'(\frac{A}{B^2})^2(A-5B) \tag{52}$$

It is easily seen that, for $\alpha' = 0$ (i.e. unnormalized Ricci flow) $(A - B)$ decreases with increasing t, but for other values of α' different from zero the scale factors evolve differently. The flow equation for $B(t)$ is

$$\frac{dB}{dt} = \left(4\frac{A}{B^2} - 20(\frac{A}{B^2})^2\right) B \tag{53}$$

If $\frac{B^2}{A} < 5$ (or $-\frac{A}{B^2} < -\frac{1}{5}$) we have

$$\frac{dB}{dt} < 0 \tag{54}$$

which explicitly shows that $B(t)$ is decreasing in this region. We then move on to the case where $\frac{B^2}{A} > 5$. Assume $p = \frac{A}{B^2}$. The quantity inside the bracket in Eq.53 is a polynomial in p, $f(p) = 4p - 20p^2$. $f(p)$ represents a parabola (upside down) and its upper bound i.e $max[f(p)] = \frac{1}{5}$ occurs at $p = \frac{1}{10} < \frac{1}{5}$. The parabola intersects the abscissa at $p = 0, \frac{1}{5}$ and progressively increases in the negative direction of the ordinate (see Fig.6). Thus, $f(p)$ is positive in the region $0 < p < \frac{1}{5}$ and, therefore $B(t)$ increases with increasing t. Outside this domain of t, $B(t)$ decreases with increasing t. We now show the above-mentioned facts numerically. In Fig[.7] we have shown the behaviour of the scale factors for different genres of $\frac{A}{B^2}$. The first figure (Fig.7(a)) has been plotted for such initial values of $A(t)$ and $B(t)$ which

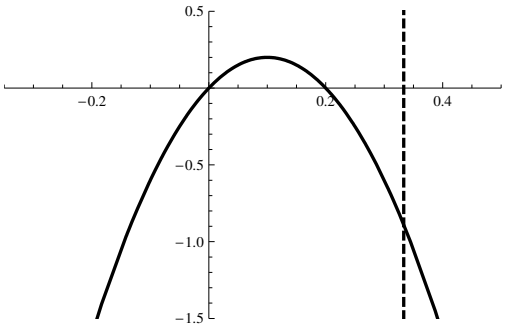

(a)$f(\frac{A}{B^2}) = 4(\frac{A}{B^2}) - 20(\frac{A}{B^2})^2$ and $(\frac{A}{B^2}) = \frac{1}{3}$

Figure 6: $f(\frac{A}{B^2})$ vs $(\frac{A}{B^2})$ for $\alpha' = 1$

correspond to $\frac{B^2}{A} < 5$, when both the scale factors are decreasing (see Eqn.[54], Fig. [7(b)]). In Fig.7(b) we have shown an interesting turning behavior where $B(t)$ initially decreases but eventually increases. The initial condition has been chosen to satisfy $\frac{A}{B^2} > \frac{1}{5}$ but during the evolution $A(t), B(t)$ decreases so that $\frac{A}{B^2}$ eventually becomes less than $\frac{1}{5}$ leading to growing nature of $B(t)$. On the other hand, for $\alpha' = -1, 0$, the evolution is easy to comprehend from the equations (Eqn.[51]). The corresponding evolution of the scale factors is shown, respectively in Fig[7(c)] and Fig[7(d)].

5. **Phase plots**

Let us now turn to the phase portraits(Fig.8).

The phase portraits in Fig.8 are for $C = B$. From these plots and the equations, it is easy to see that $A = 0$ is a fixed point of the system. For $\alpha' = 1$, trajectories from one region in phase space converge to the singularity $B = 0$ whereas others move towards the fixed point $A = 0$. The critical curve demarcating this behaviour is $\xi = BC/A = 3$ (plotted in dashed line). For $\alpha' = 0$ and $\alpha' = -1$ the flow show similar behavior with the trajectories proceed towards larger values of B and $A = 0$.

6. **Curvature evolution**

As before, here also we analyze the evolution of the scalar curvature. We have shown two different regimes of initial conditions, namely $A_0 > B_0 > C_0$ and $A_0 < B_0 < C_0$ in Fig.[9] for $\alpha' = 1$, where we note the increasing or decreasing nature of the scalar curvature (for

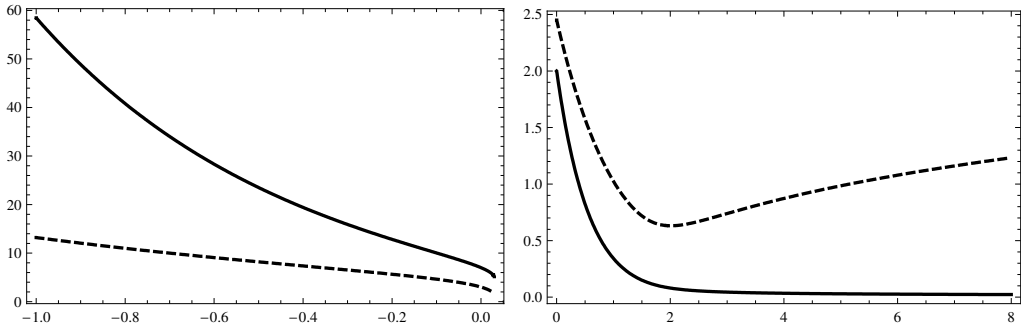

(a)$(A_0, B_0) = (7, 3), \alpha' = 1, T_s = 0.03$ (b)$(A_0, B_0) = (2, 2.45), \alpha' = 1$

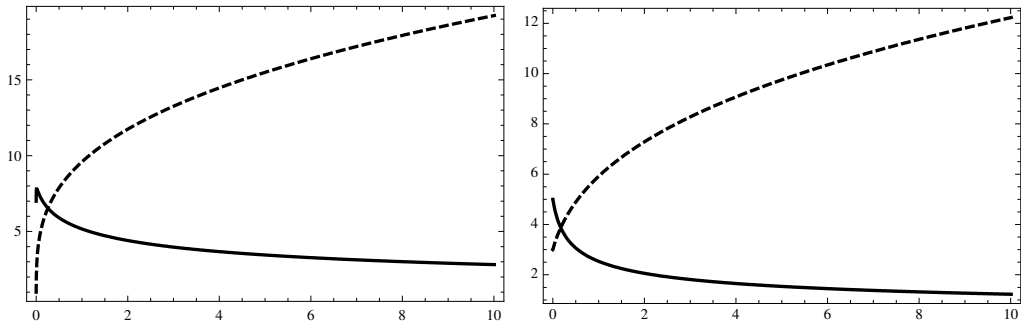

(c)$(A_0, B_0) = (7, 1), \alpha' = -1, T_s = -0.0003$ (d)$(A_0, B_0) = (5, 3), \alpha' = 0, T_s = -0.15$

Figure 7: $A(t), B(t)$ vs t for $\alpha' = 1$, $\alpha' = -1$ and $\alpha' = 0$

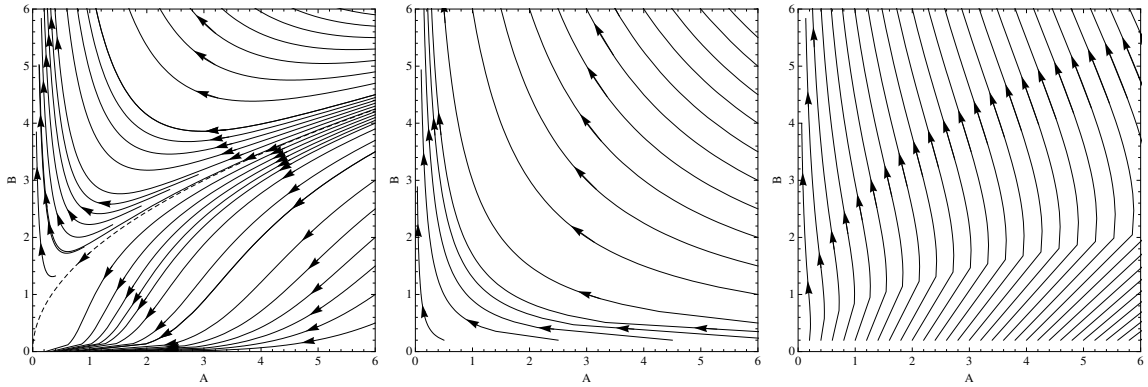

(a)$\alpha' = 1$ (b)$\alpha' = 0$ (c)$\alpha' = -1$

Figure 8: $2nd$ order flow on Nil for $B = C$

different initial conditions). For $\alpha' = 0$ and $\alpha' = -1$ the scalar curvature monotonically converges to zero asymptotically after beginning from a negative value.

We conclude this section by providing a comparison of the evolution of different scale factors and Scal. curvature for Nil manifolds in tableII.

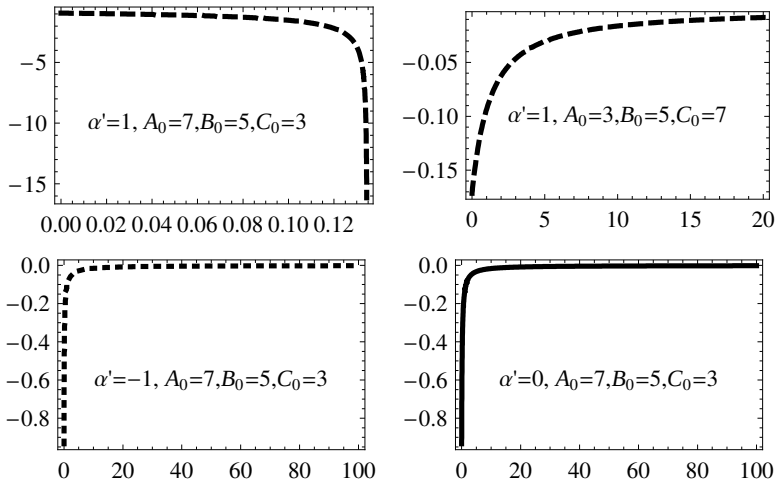

(a)Evolution of scalar curvature for various α', and A_0, B_0, C_0

Figure 9: Evolution of scalar curvature for Nil.

Table II: Comparisons of the evolution of different scale factors and Scal. curvature for Nil

	$A(t)$	$B(t)$	$C(t)$	$Scal$
$\alpha' = 0$	decreasing	increasing	increasing	asymp. flat starting from -ve.
$\alpha' = 1$	decreasing	depends on i.c	depends on i.c	increase/decrease entirely -ve, past/future asymp. flat
$\alpha' = -1$	decreasing, asymp. flat	increasing	increasing	asymp. flat starting from -ve.

C. Computation on Sol

1. Flow equations

Sol is a solvable group which has minimum symmetry among all the eight geometries. The group action in $\mathbb{R}^3$ can be written as

$$(x, y, z) \circ (x', y', z') = \left(x + e^{-z}x', y + e^{z}y', z + z'\right) \tag{55}$$

We can put left invariant vector fields[¶] on the manifold, for which the structure constants in the Milnor frame will be $\lambda = -2, \mu = 0, \nu = +2$. Sol really has a two parameter family of metrics upto diffeomeorphism (obtained by scaling and redefinition of the coordinates, see [31]). Using the values of the structure constants, we can find the components of Rc and $\widehat{Rc}^2$ tensors. The $2nd$ order flow equations reduce to,

$$\frac{dA}{dt} = \frac{-4(A^2 - C^2)}{BC} - 4\alpha' \frac{(A+C)^2(A^2 - 2AC + 5C^2)}{AB^2C^2} \tag{56}$$

$$\frac{dB}{dt} = 4\frac{(A+C)^2}{AC} - 4\alpha' \frac{(A+C)^2(5A^2 - 6AC + 5C^2)}{A^2BC^2} \tag{57}$$

$$\frac{dC}{dt} = -4\frac{(C^2 - A^2)}{AB} - 4\alpha' \frac{(A+C)^2(5A^2 - 2AC + C^2)}{A^2B^2C} \tag{58}$$

2. Numerical and analytical estimates

(a) The behaviour of the scale factors for the above higher order flow are different from those in unnormalized Ricci flow. From Fig.10(d) (unnormalized Ricci flow) we note that the scale factors do not have a future singularity. In fact, we see the appearance of a cigar degeneracy. The above behaviour can be predicted qualitatively from the equations themselves. We note that A and C can be interchanged in the equations. So instead of three equations it is enough to examine two of them. Further, without loss of generality, we may assume $A > C$. For $\alpha' = 1$ the scale factors converge (see Fig 10 (a)). If $\alpha' = 0$ and $A > C$ we find that $B(t)$, $C(t)$ increase and $A(t)$ decreases (more detail for $\alpha' = 0$ can be found in [1]). If $\alpha' = -1$ the behaviour of the scale factors bear a resemblance with unnormalized Ricci flow, though the singularity time (in the past) changes due to the higher order term (Fig.10(c) illustrates one such example for a particular set of initial values).

(b) We now consider the case $\alpha' = 1$ and analyze the evolution of the scale factor $A(t)$ a bit further. It can be shown that Eqn.56 can be written as

$$\frac{dA}{dt} \leq -4\frac{A}{C}\frac{A}{B}\left(1 - \frac{C}{A}\right)^2 - \frac{2}{B}\frac{A}{B}\left(1 - \frac{C}{A}\right)^2\left(1 + \frac{A}{C}\right)^2 - \frac{8}{B}\frac{A}{B}\left(1 + \frac{C}{A}\right)^2 \tag{59}$$

which shows that $A(t)$ is decreasing in forward time. This is also true for $C(t)$ where the second term in Eq.58 dominates over the first term and, therefore, the net effect is a

[¶] it is easy to check that one such left invariant metric will be $ds^2 = e^{2z}dx^2 + e^{-2z}dy^2 + dz^2$

decreasing $C(t)$. In the same way, we can argue that $B(t)$ is increasing (decreasing) for $A < B$ ($A > B$). Since $A(t)$ and $C(t)$ are both decreasing, they may approach each other. To show this, consider the difference $A - C$, which satisfies

$$\frac{d(A-C)}{dt} = -4\frac{(A-C)}{ABC}(A+C)^2 \ - 4\alpha'\frac{(A+C)^2(A-C)}{A^2B^2C^2}(A^2 - 6AC + C^2) \tag{60a}$$

$$\leq -4\frac{(A+C)^2}{ABC}C \ - 16\alpha'\frac{(A+C)^2}{B^2C} \tag{60b}$$

and demonstrates that the rate of change of $A - C$ is always negative. This feature is also clearly visible in Fig. 10(b). If $\alpha' = 0$, we may note that $\frac{dA}{dt} \leq -4A$ or $A(t) \leq (A_0 - 4t)$.

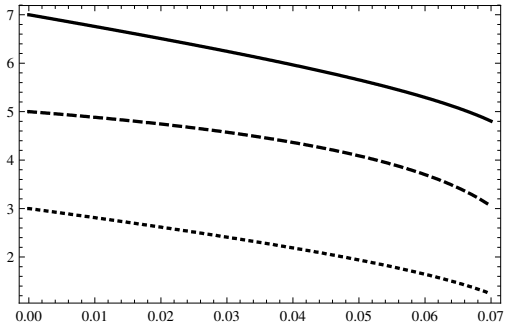

(a)$(A_0, B_0, C_0) = (7, 5, 3), \alpha' = 1, T_s = 0.078$

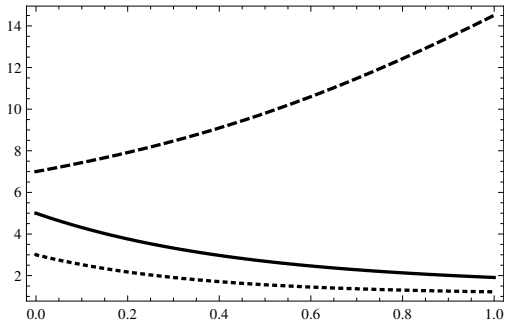

(b)$(A_0, B_0, C_0) = (5, 7, 3), \alpha' = 1$

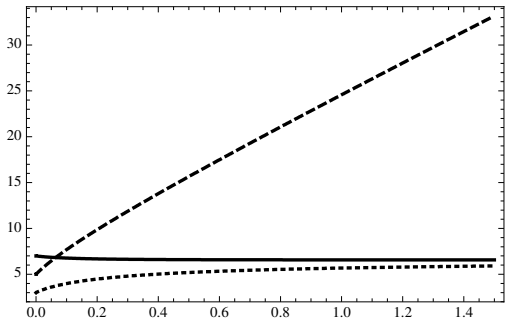

(c)$(A_0, B_0, C_0) = (7, 5, 3), \alpha' = -1, T_s = -0.052$

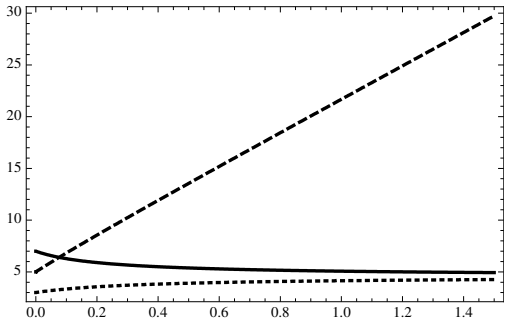

(d)$(A_0, B_0, C_0) = (7, 5, 3), \alpha' = 0, T_s = -0.154$

Figure 10: $A(t), B(t), C(t)$ vs t for $\alpha' = 1$, $\alpha' = -1$ and $\alpha' = 0$ in Sol manifold

Next we move on to a special case where $A = C$, which is analytically solvable.

3. **Special Case :** $A = C \neq B$

With this assumption, the flow equations simplify, and we have

$$\frac{dA}{dt} = -32\alpha' \frac{A}{B^2} \tag{61}$$

$$\frac{dB}{dt} = 8 - 32\alpha' \frac{1}{B} \tag{62}$$

When $\alpha' = 0$, $A(t)$ is a constant and $B(t)$ increases linearly. If $\alpha' = 1$, $A(t)$ decreases but $B(t)$ may increase/decrease depending on initial conditions (as shown in Fig 11(a),(b)). For $\alpha' = -1$, A and B both increase in forward time (Fig. 11(c)).

The flow equations can be easily solved to obtain explicit solutions as –

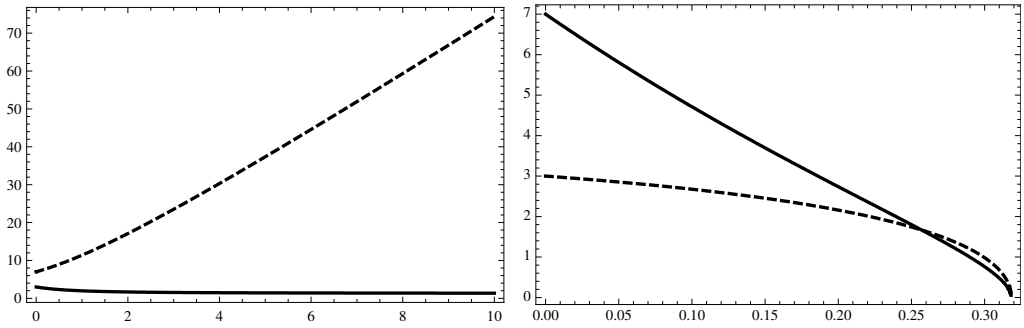

(a)$(A_0, B_0) = (3, 7), \alpha' = 1$ (b)$(A_0, B_0) = (7, 3), \alpha' = 1, T_s = 0.318$

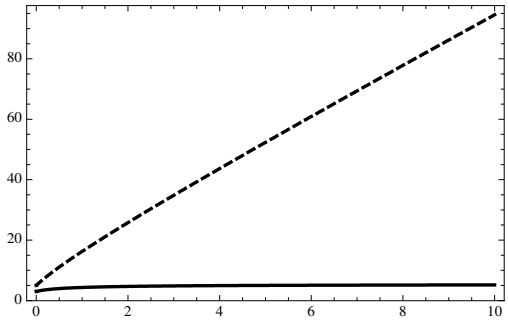

(c)$(A_0, B_0, C_0) = (3, 5, 7), \alpha' = -1, T_s =$

-0.219

Figure 11: $A(t), B(t)$ vs t for $\alpha' = 1$ and $\alpha' = -1$

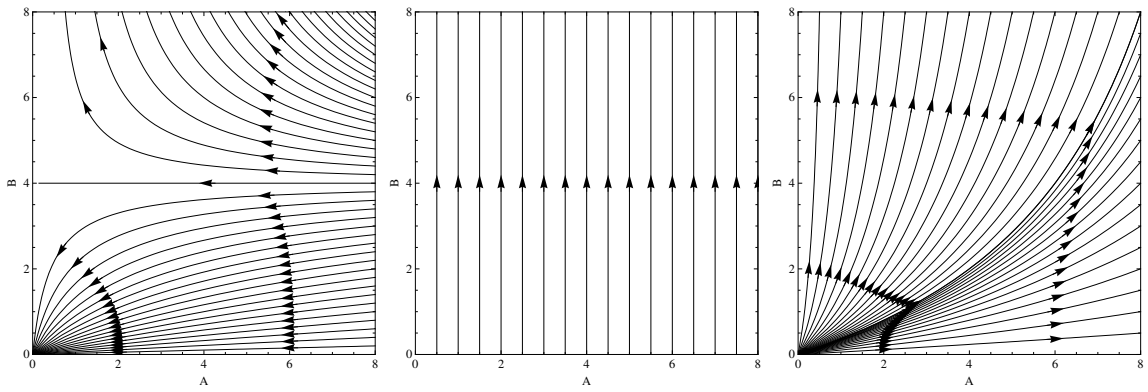

(a)$\alpha' = 1$ (b)$\alpha' = 0$ (c)$\alpha' = -1$

Figure 12: $2nd$ order flow on Sol for $A = C$

$$A\left(1 - \frac{4\alpha'}{B}\right) = \text{constant} \qquad \& \qquad B + 4\alpha' \ln|B - 4\alpha'| = 8t + k \tag{63a}$$

OR

$$A = A_0 \exp\left(-\frac{2}{\alpha'}t\right) \qquad \& \qquad B = 4\alpha' \tag{63b}$$

Note that the second solution is not valid as long as we are concerned with Riemannian manifolds.

4. Phase plots

The phase space is plotted in Fig.12. For $\alpha' = 1$ flow trajectories from $B < 4\alpha'$ converge to the singularity $B = 0$ whereas others tend towards the fixed point $A = 0$. $B = 4\alpha'$ is the critical curve in this case. For $\alpha' = 0$ flows we have $A = A_0$ and $B = 8t + B_0$, with the trajectories being straight lines flowing towards ever increasing values of B. In the $\alpha' = -1$ case the trajectories expand outwards from $A = B = 0$ to larger and larger values.

5. Curvature evolution

Lastly we examine the evolution of scalar curvature. For $\alpha' = 0$ and $\alpha' = -1$ the behavior is similar to that of Nil. The only difference appears in the $\alpha' = 1$ case where we see that the curvature increases for $C_0 < A_0 < B_0$ while it decreases in the other regime.

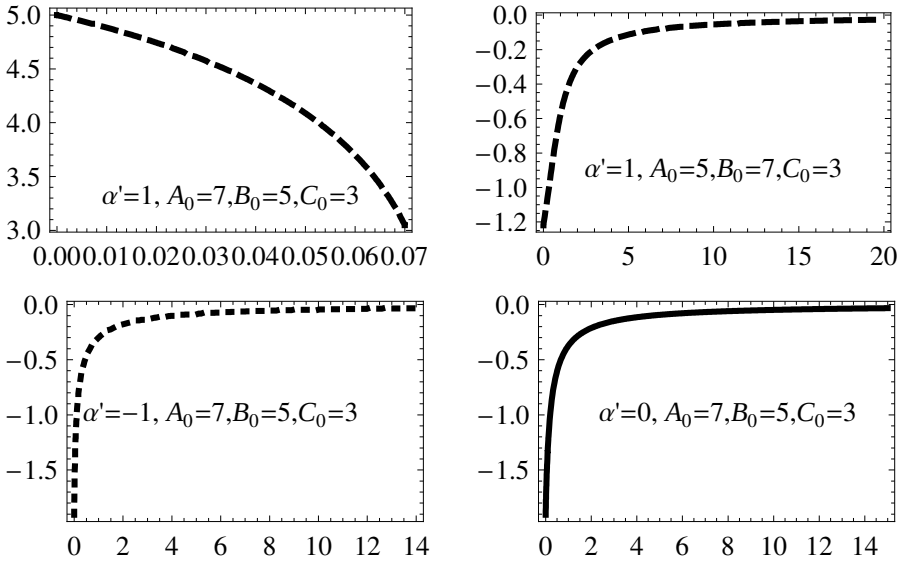

(a)Evolution of scalar curvature for various α', A_0, B_0, C_0

Figure 13: Evolution of scalar curvature for Sol.

D. Computation on $\widetilde{\text{Isom}}(\mathbb{R}^2)$

1. Flow equations

This case also involves a kind of solvable geometry. It is not mentioned in Thurston's eight geometries because it is not maximally symmetric. According to Milnor's prescription we have the structure constants as follows $\lambda = -2, \mu = -2, \nu = 0$. $\widetilde{\text{Isom}}(\mathbb{R}^2)$ also, like Sol has a two parameter family of metrics upto diffeomeorphism (see [31]). As done earlier, we can compute the various curvature quantitites and end up with the $2nd$ order flow equations given as

$$\frac{dA}{dt} = \frac{-4(A^2 - B^2)}{BC} - 4\alpha' \frac{(A-B)^2(A^2 + 2AB + 5B^2)}{AB^2C^2} \tag{64}$$

$$\frac{dB}{dt} = \frac{-4(B^2 - A^2)}{AC} - 4\alpha' \frac{(A-B)^2(5A^2 + 2AB + B^2)}{A^2BC^2} \tag{65}$$

$$\frac{dC}{dt} = \frac{4(A-B)^2}{AB} - 4\alpha' \frac{(A-B)^2(5A^2 + 6AB + 5B^2)}{A^2B^2C} \tag{66}$$

2. Analytical estimates

(a) The $\widetilde{\text{Isom}}(\mathbb{R}^2)$ class does admit Einstein metrics (flat metrics for this case) and converges under unnormalized Ricci flow(Fig.16(a)). It is easily observable that $A = B$ is the fixed

point of the flow irrespective of the presence of the higher order term. For $\alpha' = 1$ each of the scale factors attain constant value asymptotically and they are seen to decrease initially. **(b)** Let us check the evolution of each of the scale factors for $\alpha' = 1$. Using the fact that $(A^2 + 2AB + 5B^2) > (A + B)^2$ and Eqn.64 we can write the evolution of $A(t)$ as

$$\frac{dA}{dt} \leq -4\frac{(A-B)^2}{BC} - 4\frac{(A+B)^2(A-B)^2}{AB^2C^2} \tag{67}$$

So the scale factor $A(t)$ always decreases. Using the same kind of argument as earlier $(5A^2 + 2AB + B^2) > (A + B)^2$ we can rewrite Eq.65 as

$$\frac{dB}{dt} \leq 4\frac{(A+B)^2}{AC} - 4\frac{(A+B)^2(A-B)^2}{A^2BC^2} \leq 4\left(1 - \frac{(A-B)^2}{ABC}\right)\frac{(A-B)^2}{AC} \tag{68}$$

It can be easily shown that $\left(1 - \frac{(A-B)^2}{ABC}\right)$(say F_1) can be negative as well as positive. To illustrate this we assume $A = n + 2, B = n, C = n - 2$ and calculate F_1 which turns out to be $1 - \frac{4}{(n-2)n(2+n)}$. From the plot of F_1 (Fig.14), we note that depending on the value of n, F_1 can be positive as well as negative. Obviously this holds for $B(t)$ as well. Next, we estimate the behavior of $\frac{dC}{dt}$. From Eqn.66 it is easy to anticipate that $(5A^2 + 6AB + 5B^2)$ will be the deciding factor. Using the bound $-(5A^2 + 6AB + 5B^2) < -(A - B)^2$ we can recast the Eqn.66 as

$$\frac{dC}{dt} \leq 4(\frac{A}{B} - 1)^2\left(\frac{B}{A} - \frac{16B}{AC}\right) \tag{69}$$

The behaviour for $C(t)$ may be found by choosing A, B, C and calculating a quantity similar to the F_1 mentioned earlier. The evolution of $C(t)$ is qualitatively similar to that of $B(t)$.

3. **Numerical estimates**

In Fig.[15] we demonstrate our conclusions for certain specific inital values by numericaly solving the dynamical system. The cases with $\alpha' = 1$ and different sets of initial values are shown in Fig. 15(a)-(c). For $\alpha' = -1$ the flow develops a past singularity (Fig.15(d)). The nature of the evolution of scale factors for $\alpha' = 0$ is similar to the case $\alpha' = -1$ except for singularity time. These features appear in Fig. 16(a) and Fig.16(b).

4. **Special case:** $B = \eta A$

Let us now choose $B = \eta A$ with $0 < \eta < 1$. The flow equations become –

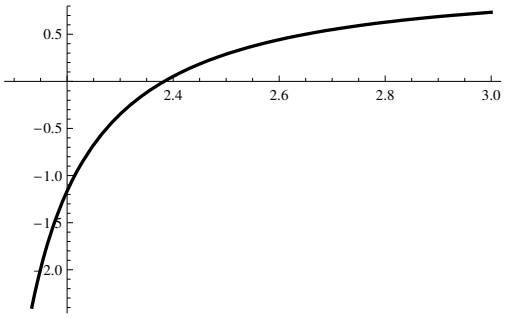

Figure 14: $F_1(n)$ vs n

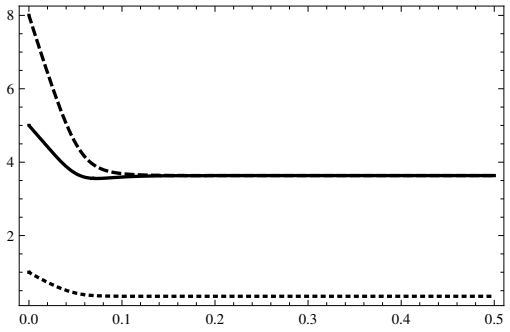

(a)$(A_0, B_0, C_0) = (5, 8, 1), \alpha' = 1$

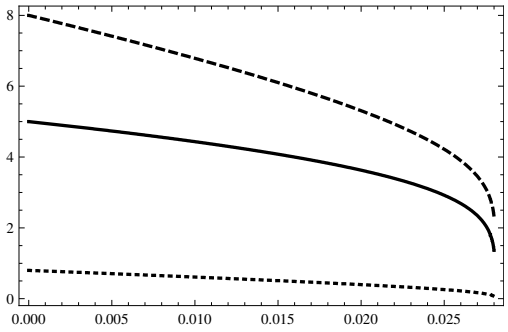

(b)
$(A_0, B_0, C_0) = (5, 8, 0.8), T_s = 0.028, \alpha' = 1$

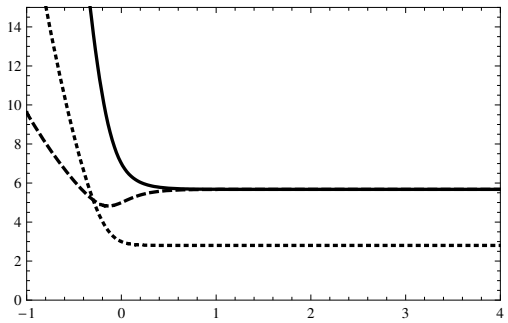

(c)$(A_0, B_0, C_0) = (7, 5, 3), \alpha' = 1$

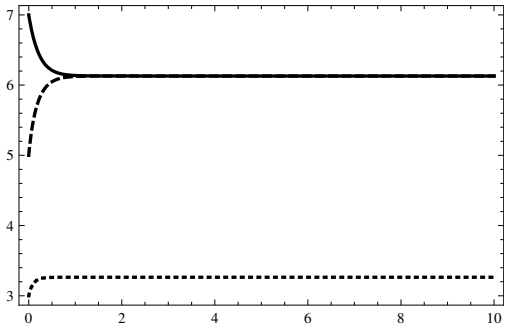

(d)$(A_0, B_0, C_0) = (7, 5, 3), \alpha' = -1, T_s = -0.128$

Figure 15: $A(t), B(t), C(t)$ vs t for $\alpha' = 1$ and $\alpha' = -1$ in $\widetilde{\text{Isom}}(\mathbb{R}^2)$

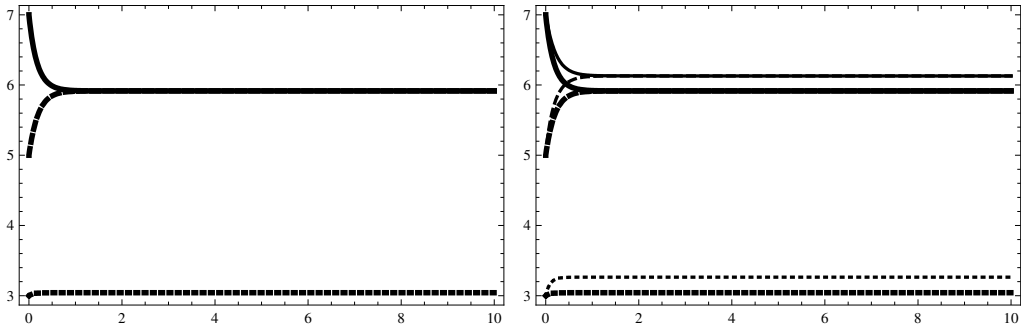

(a)$(A_0, B_0, C_0) = (7, 5, 3), \alpha' = 0, T_s = -0.3$ (b)comparison, $\alpha' = -1$, $\alpha' = 0$(thick)

Figure 16: $A(t), B(t), C(t)$ vs t for $\alpha' = 0$ in $\widetilde{\text{Isom}(\mathbb{R}^2)}$

$$\frac{dA}{dt} = 4\frac{A\,(\eta^2-1)}{C\eta} - 4\alpha'\,\frac{A(\eta-1)^2(5\eta^2+2\eta+1)}{C^2\eta^2} \tag{70a}$$

$$\frac{d\eta}{dt} = -8\,\frac{\eta^2-1}{C} + 16\alpha'\frac{(\eta+1)(\eta-1)^3}{C^2\eta} \tag{70b}$$

$$\frac{dC}{dt} = 4\frac{(\eta-1)^2}{\eta} - 4\alpha'\,\frac{(\eta-1)^2(5\eta^2+6\eta+5)}{C\eta^2} \tag{70c}$$

For $\alpha' = 0$ we can exactly solve the $\eta - C$ system and obtain a relation between $\eta(=\frac{B}{A})$ and C which is given as

$$A(t) = B(t)\frac{\left(k - \sqrt{k^2 - 4C(t)^2}\right)}{\left(k + \sqrt{k^2 - 4C(t)^2}\right)} \tag{71}$$

We substitute the above relation back in Eqn.70b and arrive at an exact solution for $\eta(t)$ as

$$\frac{2\sqrt{\eta}}{(1+\eta)} + \ln\frac{(\sqrt{\eta}-1)}{(\sqrt{\eta}+1)} = -\frac{32t}{k} + C_1 \tag{72}$$

We have analyzed numerically the $\eta - C$ system in Fig.17. We note that $\eta = 1$ is a fixed line and attracts flow trajectories in all cases. For $\alpha' = 0, -1$ all trajectories in phase space end up on $\eta = 1$. However, for $\alpha' = 1$ some flow to $\eta = 1$ whereas others flow towards the singularity at $\eta = 0 = C$.

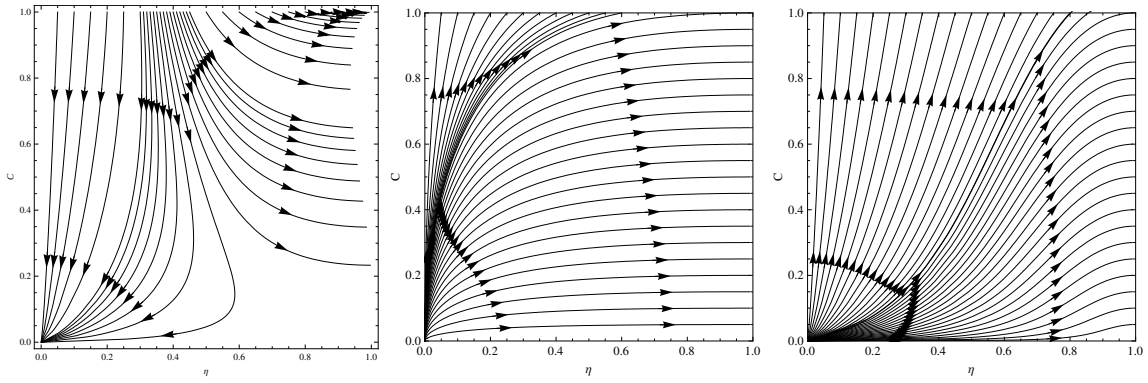

(a)$\alpha' = 1$ (b)$\alpha' = 0$ (c)$\alpha' = -1$

Figure 17: $2nd$ order flow on $\widetilde{\text{Isom}(\mathbb{R}^2)}$

5. Curvature evolution

Before we end our discussion, it is worthwhile to mention the evolution of scalar curvature for this case. Like the Sol and Nil manifolds, the scalar curvature, for $\alpha' = 0, -1$, asymptotically reaches zero but by starting from a negative value. The case $\alpha' = 1$ has different behavior depending on the initial conditions, as seen in the Fig.[18]. For some particular initial values, the scalar curvature starts from a negative value, decreases first, then asymptotically reaches zero. For the same $\alpha' = +1$, but different initial conditions, we obtain negative scalar curvature as before, but it grows to larger negative values till the flow exists.

E. Computation on $\widetilde{\mathbf{SL}(\mathbf{2}, \mathbb{R})}$

1. Flow equations

This is a three dimensional Lie group consisting of all 2×2 matrices with unit determinant and its universal cover is denoted by $\widetilde{\text{SL}(2, \mathbb{R})}$. It can be shown that $\widetilde{\text{SL}(2, \mathbb{R})}$ is not isometric to $\mathbb{H}^2 \times \mathbb{R}$ which is also a locally homogeneous space. We can put a left invariant

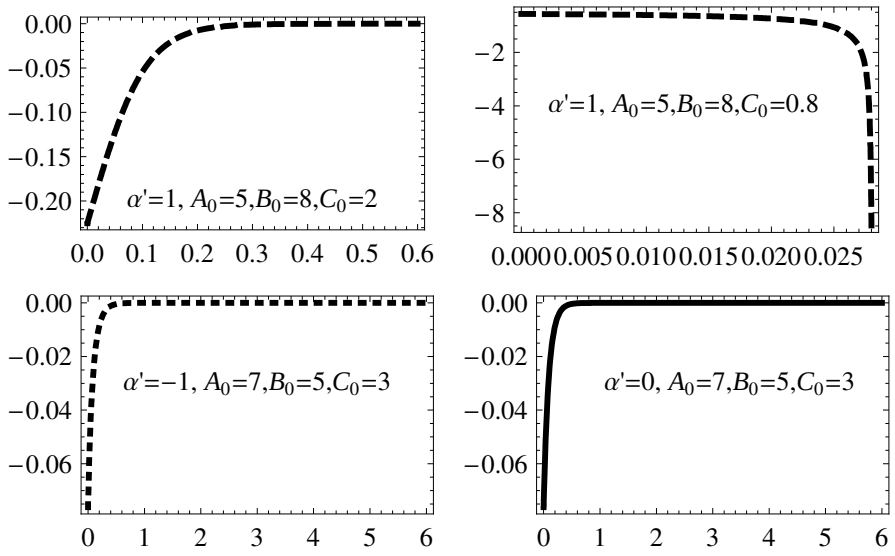

(a)Evolution of scalar curvature for various α', A_0, B_0, C_0

Figure 18: Evolution of Scalar curvature for $\widetilde{\text{Isom}(\mathbb{R}^2)}$.

metric‡ (or right invariant metric but not bi-invariant) on this manifold. Using Milnor's prescription ($\lambda = -2, \mu = -2, \nu = +2$) we find the various curvature-related quantities. The evaluated components of Rc and $\widehat{Rc}^2$ eventually lead to the following flow equations:

$$\frac{dA}{dt} = -4\frac{A^2-(B+C)^2}{BC} - 2\alpha'\frac{2(A^4+2A^2(B+C)^2-8A(B-C)(B+C)^2)}{B^2C^2A} \\ -2\alpha'\frac{2(B+C)^2(5B^2-6BC+5C^2)}{B^2C^2A} \tag{73}$$

$$\frac{dB}{dt} = -4\frac{B^2-(A+C)^2}{AC} - 2\alpha'\frac{2(5A^4+4AC(B+C)^2+A^3(-8B+4C))}{A^2C^2B} \\ -2\alpha'\frac{2(2A^2(B^2-4BC-C^2)+(B+C)^2(B^2-2BC+5C^2))}{A^2C^2B} \tag{74}$$

$$\frac{dC}{dt} = -2\frac{2C^2-2(A-B)^2}{AB} - 2\alpha'\frac{2(5A^4-4A^3(B-2C)-4AB(B+C)^2)}{A^2B^2C} \\ -2\alpha'\frac{2(-2A^2(B^2+4BC-C^2)+(B+C)^2(5B^2-2BC+C^2))}{A^2B^2C} \tag{75}$$

[‡] one such set of left invariant forms are

$$\begin{cases} \pi^1 = dx + (1+x^2)^2dy + (x-y-x^2y)dz \\ \pi^2 = 2xdy + (1-2xy)dz \\ \pi^3 = dx + (x^2-1)dy + (x+y-x^2y)dz \end{cases}$$

2. **Analytical and numerical estimates**

(a) The abovementioned equations are very hard to solve, analytically, when $\alpha' \neq 0$. For $\alpha' = 0$ we can see from Eqn.73 and Eqn.74 that the flow is symmetric in A and B. Assuming $A_0 \geq B_0$, without any loss of generality, we can show that $A(t) \geq B(t)$ throughout the $\alpha' = 0$ flow. This may be inferred (for $A > B > C$) from the evolution of the difference of $(A - B)$ given as

$$\frac{d(A-B)}{dt} = -\frac{4}{ABC}\,(A-B)\,(A+B-C)\,(A+B+C) \leq 0 \tag{76}$$

The evolution of $C(t)$ is straightforward. We note that there exists a lower bound, in the following sense,

$$\begin{aligned}\frac{dC}{dt} &= \frac{4}{AB}\big((A-B)^2 - C^2\big) \\ &= 4\Big(\Big(\frac{A}{B} + \frac{B}{A}\Big)^2 - \frac{C^2}{AB} - 2\Big) \geq -4\end{aligned} \tag{77}$$

Eqn.77 shows that $C(t)(= C_0 - 4t)$ is monotonically decreasing –a point of difference from what we find for normalised Ricci flow. Similarly, it is not difficult to show that $B(t)$ is also monotonically increasing, if we assume $A_0 > B_0 > C_0$. However, the nature of the evolution of $A(t)$ shows an increase though it is not monotonic. This can be justified as follows. We have

$$\frac{dA}{dt} = \frac{4}{BC}\,(A+B+C)\,(B+C-A) \tag{78}$$

Thus, $A(t)$ will increase monotonically provided $A < (B + C)$, otherwise it will decrease initially and then increase. We further note that as $A(t)$ and $B(t)$ increase they approach each other. This feature follows from Eqn.76, assuming $A_0 > B_0 > C_0$. We can write

$$\begin{aligned}\frac{d(A-B)}{dt} &= -\frac{4}{ABC}\,(A-B)\,(A+B-C)\,(A+B+C) \\ &\leq -\frac{4}{AB}\,(A-B)\,(A+B-C) \\ &\leq -12\frac{C}{AB}(A-B)\end{aligned} \tag{79}$$

All the above stated features for $\alpha' = 0$ are shown in Fig.19(e).

(b) For $\alpha' \neq 0$ it is difficult to understand even the qualitative nature of the evolution of scale factors, so we tried numerical solutions for some particular initial values. Before we start discussing the numerical results, let us recall that the $\widetilde{\mathrm{SL}(2,\mathbb{R})}$ class does not contain Einstein metrics. The unnormalized Ricci flow does not converge– instead it evolves towards the pancake degeneracy. But the inclusion of higher order terms seems to oppose this. For $\alpha' = 1$ the scale factors converge for different initial values -a fact depicted in Figs. (19)(a-c). On the other hand, the $\alpha' = -1$ case resembles the unnormalized Ricci flow where two of the expanding scale factors approach each other, though the past singularity time is larger (Fig.19(d)). The generic behavior of scale factors for $\alpha' = 0$ are retained for $\alpha' = -1$, except for the evolution of $C(t)$–a fact depicted in the Figs. (19)(e-f).

Finally, we move on the special case where $A = B \neq C$ where we have an exact relation between the scale factors for $\alpha' = 0$.

3. **Special case:** $A = B \neq C$

The flow equations in this case are:

$$\frac{dA}{dt} = 8 + 4\frac{C}{A} - 4\alpha' \, \frac{8A^2 + 12CA + 5C^2}{A^3} \tag{80a}$$

$$\frac{dC}{dt} = -4\frac{C^2}{A^2} - 4\alpha' \, \frac{C^3}{A^4} \tag{80b}$$

For $\alpha' = 0$ we can exactly solve the system and arrive at a relation between A and C given as

$$C(t) = \frac{A(t)^2 \; k_1 \; \exp(-A(t)^2)}{\frac{C(t)}{A(t)} + k_1 \; \exp(-A(t)^2)} \tag{81}$$

We can also check that for $\alpha' = 0$ the scale factors diverge from each other. This may be noted from the rate of evolution of the difference of scale factors, as given below.

$$\frac{d(A-C)}{dt} = 8 \; + \; \frac{C}{A} \; \left(1 + \frac{C}{A}\right) \geq 8 \tag{82}$$

For $\alpha' = -1$ we can write down the expressions for the differences of the scale factors from Eqn.80, as follows,

$$\frac{d(A-C)}{dt} = 8 \; + \; \frac{4\left(5C^2 + A^2\left(8 + C\right) + AC\left(12 + C\right)\right)}{A^3} - \frac{4}{A}\left(\frac{C}{A}\right)^3 \tag{83}$$

$$\geq 8 + \frac{4\left(A + C\right)\left(5C + A\left(C + 7\right)\right)}{A^3} \tag{84}$$

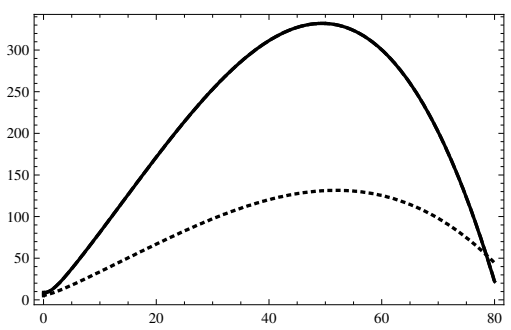

(a)$(A_0, B_0, C_0) = (9, 7, 5), \alpha' = 1$

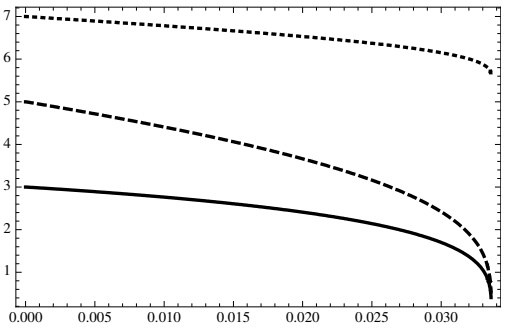

(b)

$(A_0, B_0, C_0) = (3, 5, 7), \alpha' = 1, T_s = 0.033$

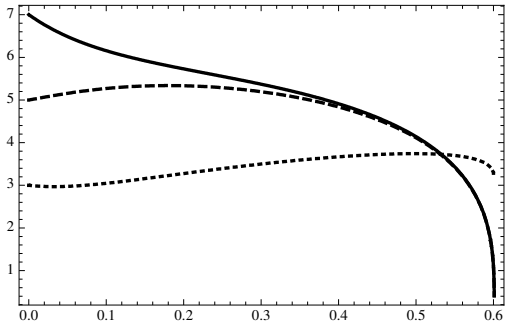

(c)$(A_0, B_0, C_0) = (7, 5, 3), \alpha' = 1, T_s = 0.6$

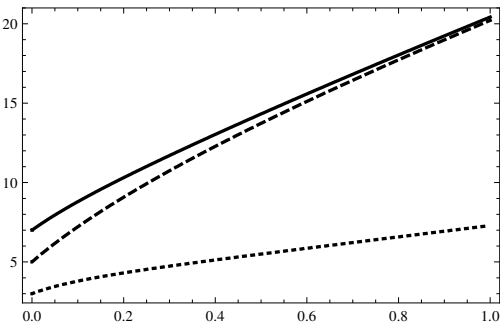

(d)

$(A_0, B_0, C_0) = (7, 5, 3), \alpha' = -1, T_s = -0.07$

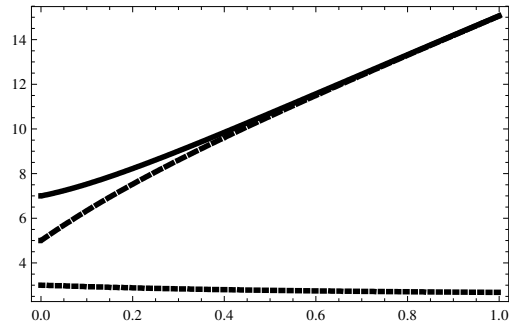

(e)

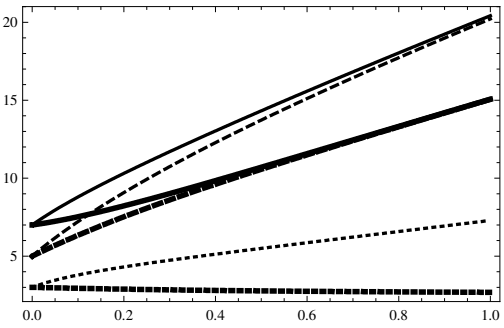

(f)$\alpha' = -1$ and $\alpha' = 0$(thick)

$(A_0, B_0, C_0) = (7, 5, 3), \alpha' = 0, T_s = -0.24$

Figure 19: $A(t), B(t), C(t)$ vs t for $\alpha' = 1$, $\alpha' = -1$and $\alpha' = 0$ for $\widetilde{\mathrm{SL}(2,\mathbb{R})}$

where we maintain $A > C$. Here the scale factors are diverging. This fact has been numerically verified in Fig.20(c). We do not show the evolution of the scale factors $A(t)$ and $C(t)$ for $\alpha' = 0$ because their nature are similar to the $\alpha' = -1$ case. Lastly, if $\alpha' = 1$, the evolution of the scale factor $C(t)$ can be found from Eqn.80b. However, the evolution of $A(t)$ will be different for different initial conditions — features which are shown in Fig.20(a)and

inFig.20(b). Let us now turn to the phase potraits.

4. **Phase plots**

As before, we plot the above–mentioned reduced system in Fig.21. For $\alpha' = 0, -1$ trajectories flow to larger values of A. But in the case of $\alpha' = 1$, the presence of a fixed point $(A, C) = (4\alpha', 0)$ makes the flow more interesting. In this case, some trajectories from a certain region in the phase space go towards larger A as before, but others converge to the singularity at $A = 0$. There also exists a critical curve, which flows into the fixed point, and demarcates the regions with different asymptotics.

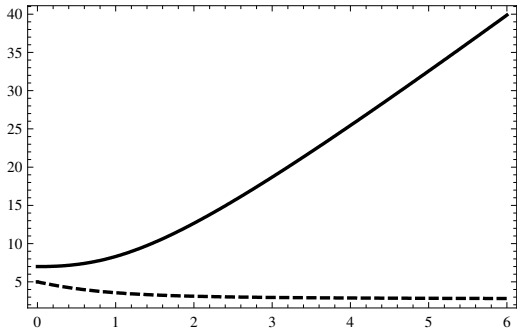

(a)$(A_0, C_0) = (7, 5), \alpha' = 1$

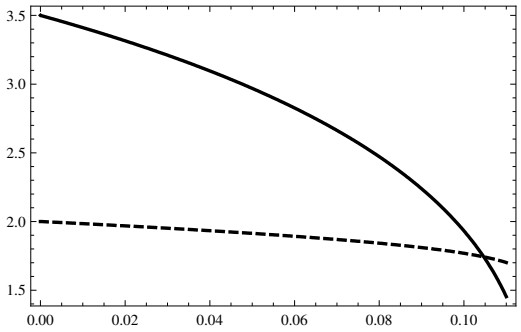

(b)$(A_0, C_0) = (3.5, 2), \alpha' = 1, T_s = 0.11$

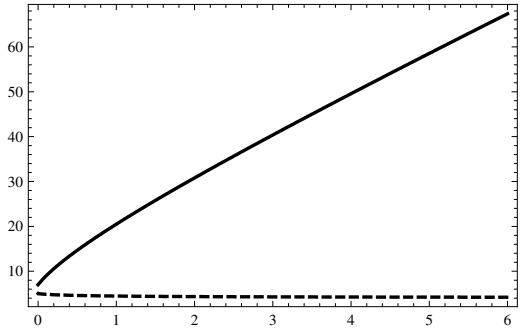

(c)$(A_0, C_0) = (7, 5), \alpha' = -1, T_s = -0.13$

Figure 20: $A(t), C(t)$ vs t for $\alpha' = 1$, and $\alpha' = -1$

5. **Curvature evolution**

We end by plotting the scalar curvature evolution. This is not very different from the earlier cases (Sol and Nil), for $\alpha' = 0$ and $\alpha' = -1$ where the curvature asymptotically goes

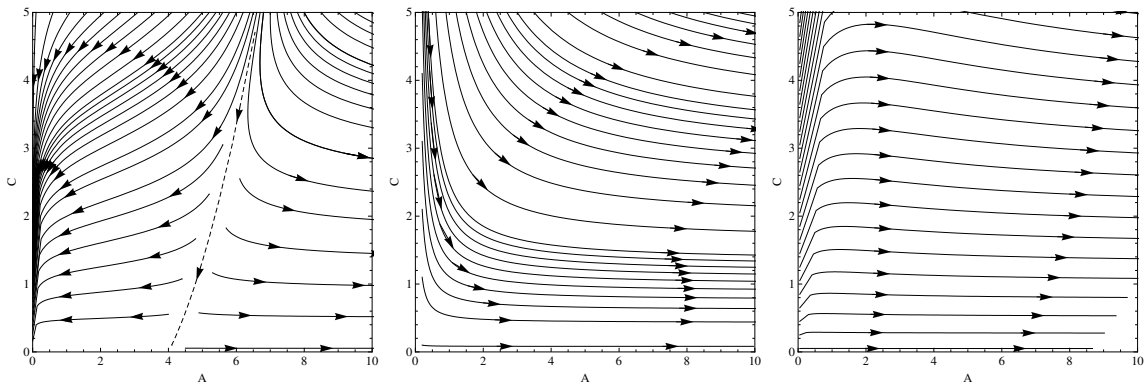

(a)$\alpha' = 1$ (b)$\alpha' = 0$ (c)$\alpha' = -1$

Figure 21: $2nd$ order flow on $\widetilde{\mathrm{SL}(2,\mathbb{R})}$ for $A = B$

to zero starting from a negative value. However, when $\alpha' = +1$ we find some interesting features which can be seen in Fig.[22]. For a particular initial condition, the scalar curvature increases from a negative value towards zero, stays there for a while and then drops to lower values once again.

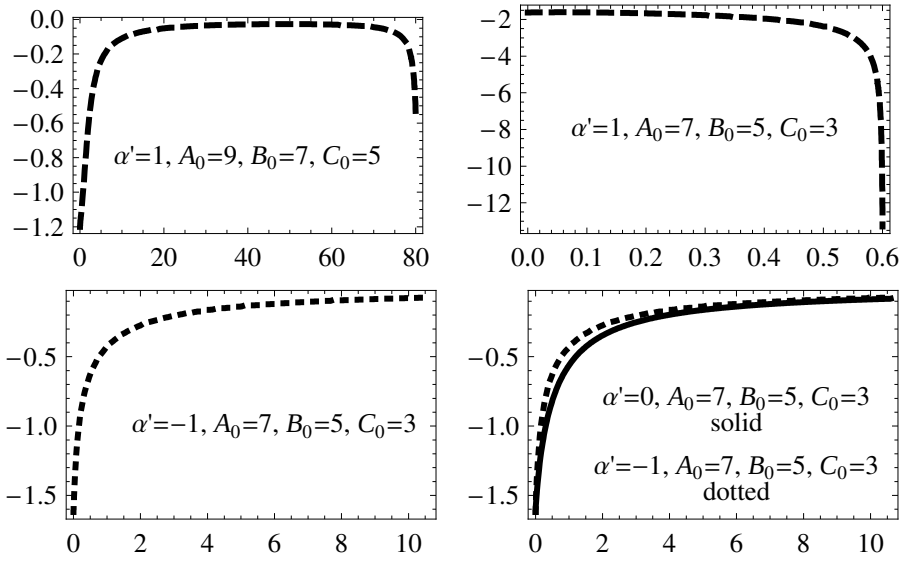

(a)Evolution of scalar curvature for various α', A_0, B_0, C_0

Figure 22: Evolution of scalar curvature for $\widetilde{\mathrm{SL}(2,\mathbb{R})}$.

V. CONCLUSIONS

Our overall aim in this work has been to study in detail the consequences of second order (in Riemann curvature) geometric flows on three dimensional homogeneous spaces, using analytical, semi-analytical and numerical methods. Through the analysis carried out, we believe we have been able to obtain quite a few characteristics which seem to arise for second order geometric flows on three dimensional homogeneous (locally) geometries. Here, we briefly summarize our results and mention a few possibilities for the future.

From our results, we can say that for manifolds which do not contain Einstein metrics the flow characteristics show new features essentially caused by the inclusion of the higher order term. On the other hand, the class of group manifolds which admit metrics of Einstein class (whether it is flat or round), results for second order flows appear to be refinements over known results for Ricci flows. However, generic new characteristics do arise with varying sign of α' –in particular, a negative α'– and these have been noted in our work.

In several restricted cases (i.e. where two of the scale factors are related), we are able to solve the flow equations exactly. We have obtained analytical solutions in such restricted cases for *Nil*, *Sol*, $\widetilde{\mathrm{Isom}(\mathbb{R}^2)}$, $\widetilde{\mathrm{SL}(2,\mathbb{R})}$ manifolds. The exact solutions are instructive because they help in obtaining analytical expressions for fixed points (curves) as well as in understanding the evolution of the scale factor. In addition, we also use them for checking our numerics.

A generic observation is the fact that the singularity time changes due to the inclusion of higher orders in the flow equations. This pattern is noticeable throughout in our numerical work.

The results for $\alpha' < 0$ are, in quite a few cases, strikingly different from those for $\alpha' = 0$ or $\alpha' > 0$. Even the evolution of the scalar curvature exhibits a different behaviour in many of the cases studied.

For $SU(2)$ all the scale factors do not converge for $\alpha' = -1$ which is exactly opposite to the characteristics for $\alpha' = 1$ and $\alpha' = 0$. Here, if $\alpha' = 0, 1$, the scalar curvature increases but when $\alpha' = -1$ it increases first and then decreases. The appearance of negative scalar curvature in $SU(2)$ is also noted. In the case for Sol manifold the behavior of the scale factors depend on different initial conditions for $\alpha' = \pm 1$—so does the evolution of the scalar curvature.

In the case of $\widetilde{Isom(\mathbb{R}^2)}$ all the scale factors converge for $\alpha' = 1$. When $\alpha' = -1$ one scale factor decreases while the other two increase. In the last case, SL(2,R), we find that for $\alpha' = 1$ all the scale factors may initially increase but they converge towards a singularity. However, for $\alpha' = -1$ all the scale factors diverge.

In all cases we have obtained the phase portraits, which we feel, helps in visualising the flow features as well as the fixed points. We also provide a summary of all our results in several tables in the sections as well as, in the end.

Among possible future directions, we mention a few below.

• It would be interesting to pursue the approach presented in [13] for such higher order flows.

• A more systematic and exhaustive analysis of the stability and classification of fixed points, which is largely an algebraic problem, can be carried out for such second order flows. This will surely shed more light on the behaviour of these flows from an analytical perspective.

• Given the fact that such three manifolds do arise in various physically relevant contexts, it will be nice to know whether our results on higher order flows can help us understand such scenarios in any meaningful way.

• The relevance of our results in the context of renormalisation group flows of the bosonic nonlinear σ-model deserve some attention.

• Since homogeneous four manifolds are already classified and studied with reference to Ricci flows [32] it would be worthwhile extending our results to four manifolds.

We hope to address some of these issues in future articles.

Table III: Comparisons of scale factors for different cases

Manifold	Bianchi Type	$\alpha' = 0$	$\alpha' = 1$	$\alpha' = -1$
SU(2)	IX	all scale factors converge to finite time singularity	different convergence rates, singularity times	does not always converge to a singularity
Nil	II	pancake degeneracy	depends on initial data	pancake degeneracy
Sol	IV_{-1}	cigar degeneracy	depends on initial data	depends on initial data
$\widetilde{\text{Isom}(\mathbb{R})^2}$	VII_0	one decreases and other two increase, converges to flat	all decrease and converge to flat	one decreases and other two increase, converges to flat
$\widetilde{\text{SL}(2,\mathbb{R})}$	VIII	one decreases and two increase	increases or decrease	all increase and diverging

Table IV: Comparisons of scalar curvature between different cases

Manifold	$\alpha' = 0$	$\alpha' = 1$	$\alpha' = -1$
SU(2)	Scal. curvature increases can be -ve.	Scal. curvature increases or decreases (entirely -ve. or +ve.)	Scal. curvature increases/decreases, can be -ve.
Nil	asymptotically goes to flat from -ve. value	increases $(A_0 < B_0 < C_0)$ or decreases $(A_0 > B_0 > C_0)$ depending on initial value	asymptotically goes to flat from -ve. value
Sol	asymptotically goes to flat from -ve. value	increases $(C_0 < A_0 < B_0)$ or decreases $(A_0 > B_0 > C_0)$ depending on initial value	asymptotically goes to flat from -ve. value
$\widetilde{\mathrm{Isom}(\mathbb{R})^2}$	starts with -ve. value, asymptotically goes to flat	starts with -ve. value, may develop singularity, asymptotically flat	starts with -ve. value, asymptotically flat
$\widetilde{\mathrm{SL}(2,\mathbb{R})}$	asymptotically goes to flat from -ve. value	depending on initial value, curvature may decrease (tend to zero) or increase	asymptotically goes to flat from -ve. value

Acknowledgments

SD acknowledges H. Seshadri, S. Panda for useful discusions and thanks the Institute of Mathematical Sciences, Chennai, India, for support through a post-doctoral fellowship.

[1] B. Chow and D. Knopf, *The Ricci flow: an introduction*, Mathematical Surveys and Monographs Vol. 110, AMS, Providence, 2004.

[2] B. Chow et. al *The Ricci flow: Techniques and Applications Part I: Geometric Aspects*, Mathematical Surveys and Monographs Vol. 135, AMS, Providence, 2007.

[3] R.S. Hamilton, *Three manifolds with positive Ricci curvature*, J. Diff. Geom. **17**, 255 (1982).

[4] D. Friedan, *Nonlinear Models in 2+ϵ Dimensions*, Phys. Rev. Letts. **45** 1057 (1980), D. Friedan,*Nonlinear Models in 2+ϵ Dimensions*, Annals of Physics **163**, 318 (1985).

[5] G. Perelman,The entropy formula for the Ricci flow and its geometric applications, Preprint math.DG/0211159

[6] M. Headrick and T. Wiseman, *Ricci flow and black holes*, Class.Quant.Grav. **23**, 6683 (2006); E. Woolgar, *Some applications of Ricci flow in Physics*, arXiv:0708.2144; J. Samuel and S. Roy Chowdhury, *Energy, entropy and Ricci flow*, Class.Quant.Grav. **25**,035012 (2008) *ibid. Geometric flows and black hole entropy*, Class.Quant.Grav.24:F47-F54 (2007); N. S. Manton, *One-vortex moduli space and Ricci flow*, J.Geom.Phys.**58**,1772 (2008); M. Carfora and T. Buchert, *Ricci flow deformation of cosmological initial data sets*. In ‘‘WASCOM 2007’’---14th Conference on Waves and Stability in Continuous Media, N.Manganaro, R.Monaco, S.Rionero (eds) World Scientific (2008), 118-127; V. Husain and S. S. Seahra, *Ricci flows, wormholes and critical phenomena*, Class.Quant.Grav.**25**,222002 (2008)

[7] T. Oliynyk, V. Suneeta and E. Woolgar, *Metric for gradient renormalization group flow of the worldsheet sigma model beyond first order*, Phys.Rev.**D76**:045001,2007; T. Oliynyk, *The second-order renormalization group flow for nonlinear sigma models in two dimensions*, Class. Quantum Grav. **26** 105020, (2009); C. Guenther, and T. A. Oliynyk, *Stability of the (Two-Loop) Renormalization Group Flow for Nonlinear Sigma Models*, Lett. Math. Phys. **84** (2008), 149-157.

[8] A. A. Tseytlin, *On sigma model RG flow, central charge action and Perelman's entropy*, Phys. Rev.**D75**, 064024 (2007)

[9] A. Sen, *Equations of motion for the heterotic string theory from the conformal invariance of the sigma model*, Phys. Rev. Lett. **55**, 1846 (1985); C. G. Callan, E. T. Martinec, M. T. Perry and D. Friedan, *Strings in background fields*, Nucl. Phys. **B262**, 593 (1985)

[10] I. Jack, D. R. T. Jones, and N. Mohammedi, *A four-loop calculation of the metric β-function for the bosonic σ-model and the string effective action*, Nuc. Phys. B**322** (1989), 431-470.

[11] K. Prabhu, S. Das and S. Kar, *Higher order geometric and renormalisation group flows*, J. Geom. and Phys. **61**, 1854 (2011)

[12] J. Isenberg and M. Jackson, *Ricci Flow of locally homogeneous geometries on closed manifolds*, J. Diff. Geom. **35** (1992), 723-741 *ibid. Ricci Flow on Minisuperspaces and the Geometry- Topology Problem*. In `Directions in general relativity:Vol1`, Cambridge University Press (1993), 166-181

[13] D. Glickenstein, T. L. Payne *Ricci flow on three-dimensional, unimodular metric Lie algebras*, Comm. Anal. Geom. **18**, 927 (2010)

[14] D. Knopf *Quasi-convergence of the Ricci flow*, Comm. Anal. Geom. **8**, 375 (2000)

[15] J. Lauret *Ricci flow of homogeneous manifolds and its soliton*, arXiv:1112.5900v1

[16] X. Cao, J. Guckenheimer, L. Saloff-Coste *The backward behavior of the Ricci and cross-curvature flows on* $\mathrm{SL}(2,\mathbb{R})$, Comm. Anal. Geom. **17**, 777 (2009)

[17] X. Cao, L. Saloff-Coste *Backward Ricci flow on locally homogeneous 3-manifolds*, Comm. Anal. Geom. **17**, 305 (2009)

[18] A. U. O. Kisisel, O. Sarioglu, B. Tekin *Cotton Flow*, Class. Qunt. Grv.**25**, 165019 (2008)

[19] X. Cao, Y. Ni, L. Saloff-Coste *Cross curvature flow on locally homogenous three-manifolds. I.*, Pacific J. Math.**236**, 263 (2008)

[20] M. Ryan and L. Shepley, *Homogeneous relativistic cosmologies*, Princeton University Press, Princeton, NJ, 1975.

[21] L. Landau, *Classical Theory of Fields*, Butterworth-Heinemann, 1975

[22] J. A. Wheeler *Our Universe: The Known and Unknown*, Am. Scientist **56-1**(1968)

[23] T. Koike, M. Tanimoto, A. Hosoya, *Compact homogeneous universes*, J. Math. Phys. **35**, 4885 (1994)

[24] P.M. Petropoulos, V. Pozzoli, K. Siampos, *Self-dual gravitational instantons and geometric flows of all Bianchi types*, arXiv:1108.0003.

[25] I. M. Singer *Infinitesimally homogeneous spaces*, Comm. Pure Appl. Math. **13**, 685 (1960).

[26] W. Thurston, *Three-dimensional geometry and topology. Vol. 1*, Princeton University Press, 1997.

[27] J. Milnor, *Curvature of the left invariants metrics on Lie Groups*, Adv. Math. **21** (1976),

293-329

[28] A.L. Besse, *Einstein Manifolds*, Springer-Verlag (1987).

[29] J. Cheeger and D. Ebin, *Comparison Theorems in Riemannian Geometry*, North Holand, 1975.

[30] A. Arvanitoyeorgos, *An Introduction to Lie Groups and the Geometry of Homogeneous Spaces*, AMS, 2003

[31] D. Glickenstein, *Riemannian groupoids and solitons for three-dimensional homogeneous Ricci and cross curvature flows*, arXiv:0710.1276v2.

[32] J. Isenberg, M. Jackson and P. Lu, *Ricci flow on locally homogeneous closed-4 manifolds*, Comm. Anal. Geom. **14**(2006), 345-386